Available online at www.sciencedirect.com

ScienceDirect

Advances in Space Research 58 (2016) 2520–2542

ADVANCES IN SPACE RESEARCH (a COSPAR publication)

www.elsevier.com/locate/asr

The development of the GSFC DORIS contribution to ITRF2014

F.G. Lemoine [a,*], D.S. Chinn [b], N.P. Zelensky [b], J.W. Beall [c], K. Le Bail [d]

[a] NASA Goddard Space Flight Center, Planetary Geodynamics Laboratory, Code 698, Greenbelt, MD 20771, USA
[b] SGT Inc., 7701 Greenbelt Road, Greenbelt, MD 20770, USA
[c] Emergent Space Technologies, 6411 Ivy Lane, Greenbelt, MD 20770, USA
[d] NVI Inc., 7527 Hanover Pkwy, Greenbelt, MD 20770, USA

Received 29 July 2015; received in revised form 7 December 2015; accepted 23 December 2015
Available online 12 January 2016

Abstract

The NASA GSFC DORIS analysis center has processed data from January 1993 to December 2014 and provided 1141 weekly solutions in the form of normal equations for incorporation into the DORIS solution for ITRF2014. The solution time series, designated as gscwd26, were based on tracking data to eleven DORIS satellites divided generally into seven-day arcs. With respect to the ITRF2008 submission (Le Bail et al., 2010), the measurement model was updated to model the beacon frequency variations at certain DORIS sites, to apply the DORIS antenna phase law for the Starec and Alcatel antennae, and to apply the antenna offset corrections in the NASA GSFC orbit determination software rather than using the data-supplied corrections. We show that computing the antenna offset corrections in the orbit determination software is superior to using the offset corrections that are supplied with the DORIS data, and that this improves the RMS of fit for SPOT-2, Envisat, SPOT-4, and SPOT-5. The updates for the force model included: (1) the development of improved nonconservative force modeling for SPOT-2, SPOT-3, SPOT-5, Envisat, and HY-2A, and (2) the application of an updated static gravity model based on GRACE and GOCE data, and weekly models of the variations in the low degree gravity field deduced independently from tracking by Satellite Laser Ranging (SLR) and DORIS. The post-ITRF2008 DORIS coordinate WRMS after the launch of Envisat and SPOT-5 is improved from 11.20 to 12.45 mm with ITRF2008 (Le Bail et al., 2010), to between 8.50 and 9.99 mm with the gscwd26 SINEX solution. The application of the DORIS antenna phase laws shifts the DORIS scale wrt DPOD2008 by +6.0 mm from 1993/01/03 to 2002/06/06, and by +11.4 mm from 2002/06/13 to 2011/10/30. The application of more detailed models of time-variable gravity reduces the slopes in the Helmert transformation parameters Tx, and Ty (w.r.t. DPOD2008) after 2005. The annual amplitude in these parameters is reduced from 3.2 mm (for Tx), 4.1 mm (for Ty), to 1.7 mm (for Tx) and 2.8 mm (for Ty).

Keywords: DORIS; Terrestrial Reference Frame; ITRF2014; Precise orbit determination; Polar motion

1. Introduction

In March 2013, the International Earth Rotation and Reference Systems Service (IERS) issued a call for participation requesting that the space geodetic techniques, Satellite Laser Ranging (SLR), Very Long Baseline Interferometry (VLBI), GNSS (Global Navigation Satellite Systems), and DORIS (Doppler Orbitography and Radiopositioning Integrated by Satellite) submit updated time series of technique-specific combinations in order to develop a new realization of the International Terrestrial Reference Frame (ITRF) (IERS, 2013). The objective was to update the previous realization of the ITRF, ITRF2008 (Altamimi et al., 2011), by processing new data and taking advantage of improvements in modeling by the each of the geodetic techniques. In response to this call, the DORIS analysis centers processed DORIS data from 1993 to 2014 with improvements to both the force and measurement models (Moreaux et al., 2016). As one of the analysis

* Corresponding author.
E-mail address: Frank.G.Lemoine@nasa.gov (F.G. Lemoine).

http://dx.doi.org/10.1016/j.asr.2015.12.043
0273-1177/Published by Elsevier Ltd. on behalf of COSPAR.

centers of the International DORIS Service (IDS), NASA GSFC updated the ITRF2008-related processing, described by Le Bail et al. (2010). A strong motivation was to contribute to the reference frame for precise orbit determination (POD) of altimeter satellites especially for TOPEX/Poseidon, Jason-1, and Jason-2 which rely exclusively or extensively on SLR and DORIS data for precise orbit determination (e.g., see Cerri et al., 2010; Lemoine et al., 2010; Zelensky et al., 2010a). The primary products of our work were weekly solutions for DORIS station coordinates and Earth orientation parameters (polar motion) from January 1993 to December 2014, derived solely from DORIS data. The final solution series, gscwd25 and gscwd26, were submitted in Solution Independent Exchange (SINEX) format to the Combination Center of the International DORIS Service (IDS) and to the IDS Data Centers, in particular the NASA Crustal Dynamics Data Information System (CDDIS) (Noll and Soudarin, 2006; Moreaux et al., 2016), however it was gscwd26 that was finally included in the IDS Combination for ITRF2014.

Working in concert with the IDS Analysis Working Group (AWG), we incrementally implemented a series of changes in the measurement modeling, the force modeling, and in the data processing. We also processed new satellite data not available for ITRF2008, including data from Jason-2, Cryosat-2 and HY-2A. As in Le Bail et al. (2010) we processed all the data with the NASA GSFC Orbit Determination and Geodetic Parameter Estimation (GEODYN) software (Pavlis et al., 2015). We analyzed exclusively the DORIS range-rate data (ftp://ftp.ids-doris.org/pub/ids/data/doris22.fmt). We organize this paper by providing a thematic rather than a chronological summary of the work performed. In Section 2, we give an overview of the changes in the models, and summarize the different SINEX series where we incrementally implemented and tested different model changes. In Section 3 we describe the alterations to the nonconservative force modeling for a number of the DORIS satellites. In Section 4, we describe the modifications to the DORIS measurement model that we implemented for ITRF2014. These included the proper modeling of the beacon frequency variations, the application of the phase law for the Starec and Alcatel antennae, and the use of GEODYN-computed spacecraft antenna offset and ground antenna eccentricity offset corrections rather than using the values supplied with the DORIS data. In Section 5, we discuss the processing of the SAA-corrected data on Jason-1 and SPOT-5, and the testing of changes in the parameterization of the empirical acceleration parameters. In Section 6 we summarize the final results with respect to the WRMS, and other indices of solution quality.

2. Summary of SINEX solutions and model changes

In Table 1 we summarize the final processing standards for both series that were submitted for ITRF2014. This table can be compared directly to Table 2 of Le Bail et al. (2010). We discuss the geopotential model changes and the updates to the nonconservative force modeling in Section 3. The changes from the GOT4.7 to GOT4.8 tide model involved corrections in the S_2 tidal coefficients (Ray, 2013, see Appendix A). The processing used the DPOD2008 station coordinates (Willis et al., 2015, obtained from http://www.ipgp.fr/willis/DPOD2008/). An important change concerned the adoption of the IERS2010 model for the motion of the pole (Petit and Luzum, 2010, See Table 7.7, pp. 115). The updates to the troposphere modeling were tested by Zelensky et al. (2010b) for Jason-1 and Jason-2. We adopted the GMF mapping function (Boehm et al., 2006) instead of the Niell mapping function (Niell, 1996) used for ITRF2008. Although the Vienna Mapping Function (VMF1) (Boehm and Schuh, 2004) has now been implemented in GEODYN, the testing was not completed before the deadline for the delivery of the ITRF2014-related SINEX files.

For ITRF2014, we processed DORIS data to four new satellites: Jason-1, Jason-2, Cryosat-2 and HY-2A. We also processed data for Saral, but we did not include the Saral data in our weekly solutions since we had not yet validated the satellite-specific modeling. The NASA GSFC analysis of the Saral data is discussed by Zelensky et al. (2016). In order to verify the data processing for the new satellites, we processed both the SLR and DORIS data, analyzing the SLR and DORIS residuals, and intercomparing the SLR+DORIS and the DORIS-only orbits. The Jason-2, Cryosat-2 and the HY-2A spacecraft use the DGXX receiver, which can track up to seven DORIS beacons simultaneously (Auriol and Tourain, 2010), vastly increasing the quantity of DORIS tracking data. In addition, we re-imported data that was reissued for SPOT-4 (1998–1999), Envisat (2002–2006), Jason-2 (2008–2011), and Cryosat-2 (2010–2011). As discussed in the relevant DORISMAILs, these data releases corrected problems in the previous versions of the data.

In GEODYN we used the DORIS satellite antenna offsets described by the CNES (Cerri and Ferrage, 2013), where information about the variations in the vector position of the center of mass in the spacecraft coordinate sytem were obtained from the IDS data centers (Noll and Soudarin, 2006). For SPOT-3, the defined coordinates of the center of mass coincided with the center of the spacecraft coordinate system and no information about these variations was available.

In Table 2 we summarize the SINEX series we developed as part of our preparations for ITRF2014, and to which we refer to specifically in this paper. The previous ITRF2008-based series was gscwd12. In gscwd15, the first step in the processing was to review all the arc setups, including the start and stop times for the multi-day arcs, and make sure they coincided with the start and stop times of available data. In addition, the DORIS data were reedited. The improvements to the macromodels for some satellites were tested in the series, gscwd17. The implementation of the

Table 1
Processing standards and data for the final SINEX series delivered for ITRF2014 (gscwd25 and gscwd26). Major changes in the measurement and force modeling with respect to ITRF2008 are shown in bold.

Model	ITRF2014
Static gravity ‡	GOCO02S ($L > 5$) (Goiginger et al., 2011)
Time-variable gravity ‡	5×5 weekly time series Annual terms from GRACE ($L > 5, L \leqslant 20$)
Atmospheric gravity	ECMWF-6hr
Ocean Tides ‡	GOT4.8
Ocean Loading ‡	GOT4.8
Station coordinates	DPOD2008. (Willis et al., 2015)
Pole modeling ‡	IERS2010. (Petit and Luzum, 2010)
Troposphere model	Saastamoinen
Troposphere mapping function ‡	GMF. (Boehm et al., 2006)
A priori Met. data	GPT. (Boehm et al., 2007)
Troposphere bias adjusted ‡	Wet bias per pass
Non-conservative forces	
Atmosphere Density model	MSIS86 (Hedin, 1987)
Satellite Macromodel changes ‡	SPOT-2 & 3; Envisat
SPOT-5 solar array pitch ‡	Modeled
Spacecraft attitude	Attitude law or quaternions
Quaternions for satellite attitude	Jason-1, Jason-2, Cryosat-2 & some TOPEX arcs
DORIS measurement model	
Antenna offset corrections ‡	Computed in GEODYN using attitude law or quaternions
DORIS time bias (TOPEX) ‡	Model from SLR + DORIS orbit determination solutions
Beacon Frequency offset from nominal ‡	Modeled
Phase law for DORIS ground antennae ‡	Applied
Reissued or corrected data	
SPOT-4	1998–1999 (DORISMAIL 0801)
Envisat	2002–2006 (DORISMAIL 0823)
New data for GR3B, GAVB	(DORISMAIL 0750)
SPOT-5 SAA-corrected data	2006 to 2014 (per AWG)
New satellite data	
	Jason-1 (SAA-corrected) (2004–2008) Jason-2 (2008–2014) Cryosat-2 (2010–2014) HY-2A (2012–2014)

‡ Modeling updated for ITRF2014 compared to Le Bail et al. (2010).

model of the beacon frequency variations was tested in the series, gscwd18. The series gscwd20 was an important milestone, because therein we validated the implementation of the IERS2010-related pole modeling, and modified the atmospheric drag modeling for certain time periods following the recommendations of the Analysis Working Group (Moreaux et al., 2016). During periods of exceptionally high solar flux (F10.7) or magnetic indices (Ap), we adjusted drag coefficients every one to two hours for the SPOT satellites and Envisat. The Starec and Alcatel antennae phase law were implemented with the gscwd21 series. The final series, gscwd25 and gscwd26 used a time-series of 5x5 spherical harmonic coefficients derived from SLR and DORIS tracking to model the time-variable gravity variations from 1993 to 2014 (Lemoine et al., 2014). We delivered gscwd25 and gscwd26 to the IDS Combination Center and the IDS data centers for ITRF2014.

3. Force modeling improvements

We were strongly motivated to consider improvements to the nonconservative force modeling and the geopotential modeling for the DORIS satellites. Mismodeling of radiation-pressure related forces can induce unwanted draconitic-type signals in the satellite orbits and in the geophysical products, such as the geocenter, the station coordinates, or the earth orientation parameters (e.g. see Gobinddass et al., 2009; Cerri et al., 2010). Regarding the static geopotential, the model used for ITRF2008, EIGEN-GL04S1 (Förste et al., 2008), was based on only two years of GRACE and LAGEOS data from 2003 to 2005, so it was effectively tuned to the mean gravity field in those years. In addition, the parameterization of time-variable gravity was quite parsimonious, and relied on forward modeling the secular rates of only select terms of the

Table 2
Summary of GSFC SINEX series developed since ITRF2008.

Series	Description
gscwd10	ITRF2008 series (Le Bail et al., 2010)
gscwd12	Previous operational series (continuation of series from Le Bail et al. (2010))
gscwd15	New time series (1992–2012) Updates, data cleanups, changes in data editing
gscwd17	Test of macromodel-related changes only (SPOT-2, SPOT-3, Envisat)
gscwd18	New time series (1992–2012). Test modeling to handle changes in the nominal frequency at DORIS stations
gscwd20	New time series (1992–2013). Implementation of IERS2010 Changes to drag modeling per AWG (Toulouse, April 2013)
gscwd21	Implementation of Starec phase law
gscwd22a	Test of use of SLR-derived DORIS time bias for TOPEX
gscwd23	Test of implementation of new time-variable gravity model
gscwd25	New time series (1992–2014). Use GSFC-derived TVG solution Add Jason-1, HY-2A
gscwd26	Used in ITRF2014. Same as gscwd25, but adjust cross-track once-per-revolution (OPR) empirical accelerations per arc instead of per day Along-track OPR empirical acceleration parameterization unchanged

geopotential (e.g. C_{20}, C_{30}, C_{40}, C_{21} and S_{21}). Cerri et al. (2010) showed that already starting in 2010, for Jason-2 the EIGEN-GL04S1 gravity produced biases and drifts compared to Jason-2 orbits computed with a time series of geopotential solutions developed from GRACE (e.g. Bruinsma et al., 2010) (see in particular Figs. 13 and 14 of Cerri et al. (2010)). For this reason, we were motivated to explore alternate approaches, and we developed our own low-degree modeling of the geopotential from 1993 to 2014 using a time series. As a base mean model, we used the static geopotential model, GOCO2s, which was developed using both GRACE and GOCE data (Goiginger et al., 2011). More detail of the time-variable gravity modeling used for the different SINEX series is provided in the Supplementary Material to this paper. We note that the proper modeling of the geopotential for altimeter satellite orbits has been studied by Zelensky et al. (2011) and Rudenko et al. (2014), and is also discussed by Zelensky et al. (2016) in the context of precise orbit determination for Saral.

3.1. The nonconservative forces

We assessed the fidelity of the nonconservative force models as applied for ITRF2008 (Le Bail et al., 2010), by analyzing the amplitude of the daily along-track once-per-revolution (OPR) empirical accelerations. In Table 3 we summarize the average and median of the daily amplitudes of these accelerations over the entire set of arcs for each satellite. The NASA GSFC macromodel for SPOT-2 was derived by Gitton and Kneib (1990). For ITRF2008, we applied two tuned values of the solar radiation reflectivity coefficient $C_r : C_r = 1.0386$, for 1993–2002, and $C_r = 1.0716$, for 2003–2008 (Le Bail et al., 2010). For the initial assessment shown in Table 3 we adopted a uniform value of $C_r = 1.0386$. The Jason-2 macromodel was originally provided by the CNES and tuned by Zelensky et al. (2010a). For Cryosat-2, we used the CNES 7-plate macromodel that approximately represents the spacecraft as a trapezoidal prism (Cerri and Ferrage, 2013).

Table 3
Daily OPR along-track acceleration summary for the gscwd15 series. The average, and median of the daily acceleration amplitudes are shown over the indicated time interval in units of 1.0×10^{-9} m/s^2.

Satellite	Dates	Average	Median
TOPEX	1992–2004	0.88	0.55
SPOT-2	1992–2009	1.69	1.34
SPOT-3	1994–1996	3.14	2.82
SPOT-4	1998–2012	1.15	0.75
SPOT-5	2002–2012	0.93	0.62
Envisat	2002–2012	10.5	9.38
Jason-2	2008–2012	1.31	1.04
Cryosat-2	2010–2012	2.79	2.76

We saw immediately that the implementation of the Envisat surface modeling was questionable as the magnitude of the accelerations was much larger than for the other satellites. Although GEODYN uses the University of College London special radiation model for Envisat (Sibthorpe, 2006), a macromodel is still required to compute the accelerations due to the other surface forces (atmospheric drag and planetary radiation pressure). We applied a ten-plate macromodel for Envisat that included the Synthetic Aperture Radar (SAR) antenna for Envisat, as well as the solar array. We corrected an error in the orientation of the solar array in our earlier processing for the Envisat data. In addition, within the UCL Envisat model as implemented in GEODYN, we corrected the specification of the surface area for thermal re-radiation of the solar array. Finally, we tuned the solar radiation reflectivity coefficient (C_r) for the UCL model to 1.00417. With these

Table 4
Daily OPR along-track and cross-track acceleration summary for SPOT-2, SPOT-3, Enivsat, and HY-2A, before and after macromodel tuning, over the indicated time interval in units of 1.0×10^{-9} m/s^2.

Satellite	Nplates	Along-track OPR		Cross-track OPR		C_r
		Mean	Median	Mean	Median	
January 2004 to October 2005						
Envisat (a priori)	10	10.29	9.98	2.57	2.20	1.00
Envisat (updated)	10	1.10	1.03	1.95	1.63	1.00
Envisat (updated)	10	1.08	1.01	1.95	1.62	1.00417
Envisat (8-plate)	8	1.57	1.48	1.96	1.63	1.00
January 1993 – January 1997						
SPOT-2 (a priori)	8	1.55	1.38	3.01	2.51	1.0386
SPOT-2 (updated)	8	0.74	0.55	3.02	2.70	1.0000
February 1994 – November 1996						
SPOT-3 (a priori)	8	3.20	3.13	2.47	2.20	1.00
SPOT-3 (updated)	8	0.60	0.59	2.40	2.15	1.00
November 2011 – October 2012						
HY-2A (a priori)	6	31.5	10.1	23.4	2.9	1.146
HY-2A (updated)	6	2.41	0.65	5.79	2.60	1.000

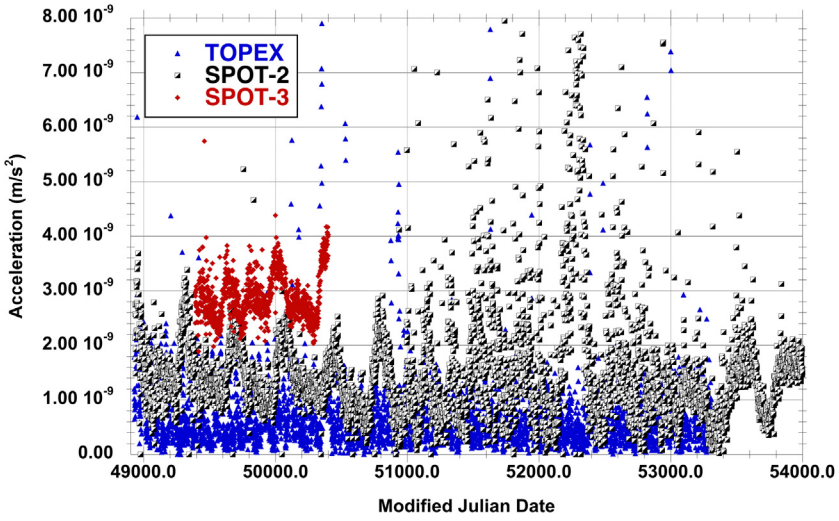

Fig. 1. TOPEX, SPOT-2, and SPOT-3 daily Along-track once-per-revolution empirical acceleration amplitude (November 1992 – November 2004) for the gscwd15 series. The SPOT-2 and SPOT-3 results are shown before retuning the SPOT-2 and SPOT-3 macromodels.

corrections, the empirical accelerations for Envisat were now more consistent with the amplitudes seen by the other satellites. The ten-plate macromodel produced lower residual along-track accelerations by about fifty percent than the eight-plate macromodel from Cerri and Ferrage, 2013 (see Table 4), indicating that the atmospheric drag and planetary radiation pressure perturbations are better accommodated when the SAR antenna geometry is taken into account in the macromodel.

In Fig. 1 we show the daily along-track OPR acceleration amplitudes from November 1992 to November 2004. We see that the TOPEX residual empirical accelerations are small and well-behaved. The SPOT-2 and SPOT-3 accelerations showed annual signals and amplitudes larger than those seen on TOPEX during periods of lower solar activity (i.e. Modified Julian Date (MJD) 49500 to 51000), consistent with a possible beta-prime or draconitic signal for these sun-synchronous satellites. Thus, we were motivated to try and tune the macromodels for these spacecraft. As shown in Fig. 2, the residual along-track accelerations for SPOT-4 and SPOT-5 were reasonable, so we did not alter the macromodels for those satellites from Le Bail et al. (2010).

From the time history of the residual along-track accelerations (Fig. 2), all the SPOT satellites show larger residual accelerations in periods of more intense solar activity (July 1998 to April 2003 or Modified Julian Date (MJD) 51000 to 52750). The higher solar activity is associated with increased atmospheric density at the satellite altitudes. The peak in solar activity from October 2001 to March 2002 (MJD 52200 to MJD 52350) is particularly pronounced. The high drag accelerations on the SPOT satellites are

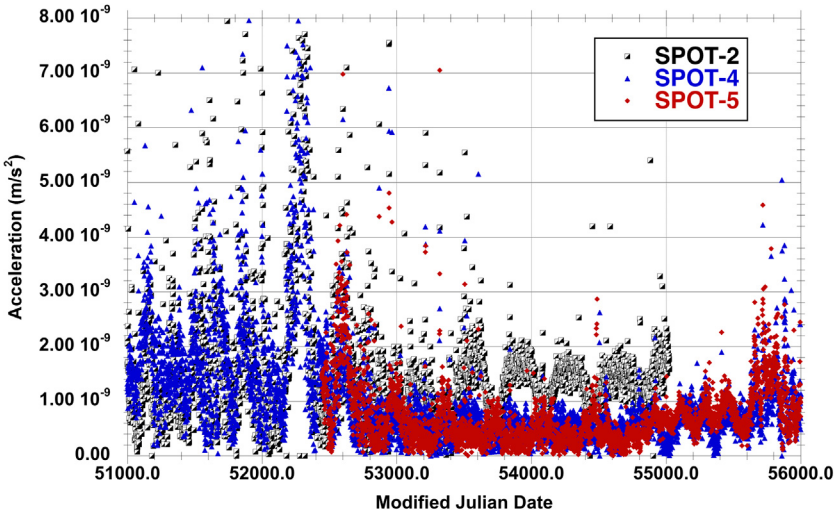

Fig. 2. SPOT-2, SPOT-4 and SPOT-5 daily Along-track once-per-revolution empirical acceleration amplitude (July 1998 to March 2012) for the gscwd15 series. The strong peak in the empirical acceleration amplitudes for SPOT-2 and SPOT-4 occurs between MJD 52200 to 52350 (October 2001 to March 2002).

not accommodated properly in the atmospheric density modeling. Seeking an improvement for the MSIS86 model (Hedin, 1987) applied to the previous ITRF2008 DORIS processing of Le Bail et al. (2010), we tested the DTM2012 atmosphere density model (Bruinsma et al., 2012, www.atmop.eu). In our tests, we applied DTM2012 to the orbit determination of the GEOSAT Follow-On spacecraft (GFO-1). The GFO-1 spacecraft was located in an orbit at 800 km altitude, similar to the SPOT satellite altitude albeit at a different inclination (~108° for GFO-1 compared to ~98° for the SPOT spacecraft). GFO-1 is an altimeter satellite tracked by satellite laser ranging (SLR) and Tranet-style Doppler that was heavily affected by atmospheric drag early in its mission (Lemoine et al., 2006). We did not notice any improvement in the SLR RMS of fit for GFO. In fact during severe solar storms, such as the "Halloween" storm of October 2003, we noticed a degradation in the SLR residuals. Although the DTM2012 model incorporated atmosphere density information from CHAMP and GRACE (deduced from accelerometer measurements), the atmosphere density from DTM2012 computed at the GFO altitude did not appear to offer an improvement over MSIS86 (Hedin, 1987). A possible reason for this performance was cited by Bruinsma (2014) who reported that the DTM model lacks data at 800 km altitude, and has no density or atmosphere data for altitudes above 1000 km. Since we had many other modeling issues to address, we chose to retain the MSIS86 model for atmosphere density modeling of the DORIS satellites.

In Table 4 we summarize the average and median daily amplitude of along-track and cross-track accelerations for the initial and final macromodels that we used. We followed the procedure used in Le Bail et al. (2010) to tune the macromodels for SPOT-4 and SPOT-5. First we adjusted the specular reflectivity coefficient of the solar array, and then, depending on the sensitivity of the combined normal equations for the macromodel parameters, we also adjusted a parameter on a surface that was orthogonal to the solar array. Solutions with unrealistic estimates for the macromodel parameters were rejected. We tested different orbit determination solutions to determine which produced the lowest value of the empirical accelerations before obtaining the final results shown in Table 4.

For SPOT-2 we adjusted the specular reflectivity of the solar array from 0.223 to 0.310, and the specular reflectivity of the −Y panel from 0.579 to 0.679. To avoid contamination by high atmospheric drag conditions, the macromodel parameters were adjusted using data only from 1993 to 1997. For SPOT-3 we adjusted the specular reflectivity of the solar array from 0.273 to 0.336 using nearly all the available data from 1994 to 1996. For HY-2A, we used data from November 2011 to October 2012 to adjust the specular reflectivity of the +Y panel (which according to Cerri and Ferrage (2013) faces the Sun) from an a priori of 0.0 to 0.221. In addition we adjusted the diffuse reflectivity of the +X panel (along-track according to Cerri and Ferrage (2013)) from 0.970 to 0.564. In addition, although the IDS AWG initially recommended a C_r of 1.146 for HY-2A, we reset this value to unity when we estimated the HY-2A macromodel parameter corrections.

3.2. Time-variable gravity

To model the time-variable gravity (TVG) variations, we used a gravity coefficient time series to degree and order 5 derived from the tracking of 21 satellites tracked by SLR and DORIS over the time period 1993 to 2014 (Lemoine et al., 2014). We give here only a brief synopsis of this time-series solution: A more detailed summary is available in the Supplementary material to this paper. The satellites that contributed to the solutions included the SLR

Table 5
POD SLR and DORIS RMS of fit Summary for SLR/DORIS standards using the modeling standards applied for the gscwd12 (ITRF2008), gscwd20 (interim product), gscwd25 (final ITRF2014 delivery) SINEX series (cm for SLR; mm/s for DORIS).

Satellite	Data	gscwd12	gscwd20	gscwd25
Dates		Jan. 2009 – June 2012	Nov. 1992 – Dec. 2014	Nov. 1992 – Dec. 2014
Lageos-2	SLR	0.881	0.823	0.815
Stella	SLR	1.600	1.472	1.388
Starlette	SLR	1.586	1.494	1.344
Larets	SLR	1.607	1.465	1.357
TOPEX	SLR	1.701	1.668	1.701
	DORIS	0.513	0.513	0.512
Envisat	SLR	1.272	1.126	1.039
	DORIS	0.494	0.491	0.491
Jason-2	SLR	1.215	1.172	1.118
	DORIS	0.361	0.379	0.379
Cryosat-2	SLR	2.131	1.304	1.134
	DORIS	0.437	0.402	0.400

cannonball satellite (Lageos-1 & 2, Starlette, Stella, Ajisai, Larets, Blits, Lares), the altimeter satellites (TOPEX, Jason-1, Jason-2, Envisat, Cryosat-2, and HY-2A), and the SPOT satellites (SPOT-2, 3, 4). The degree two terms, and the sectorals are well resolved, but C_{31} & C_{32} have poor correlation with independent solutions derived from GRACE data. The solutions were developed weekly from the combination of normal equations of the satellite data, and then smoothed using a 35-day (five week) window.

In Table 5 we summarize the SLR and DORIS RMS of fit for different satellites that used the standards associated with the SINEX series gscwd12 (continuation of ITRF2008), gscwd20 (many updates, including IERS2010 for the modeling of the pole), and gscwd25 (use of SLR-DORIS weekly time-variable gravity 5×5 time series instead of the smoothed parameter fit for the gravity field). Specifically, gscwd12 used EIGEN-GL04S1 (Förste et al., 2008); gscwd20 used GOCO2s as a background model, and annual, semiannual, and secular rates for some terms of a fit to a preliminary SLR + DORIS 4x4 time-variable gravity time series; gscwd25 used the SLR + DORIS derived 5x5 spherical harmonic coefficient time series. With this set of satellites, including the SLR cannonball satellites, we can track the improvement in orbit determination performance as the different series were developed.

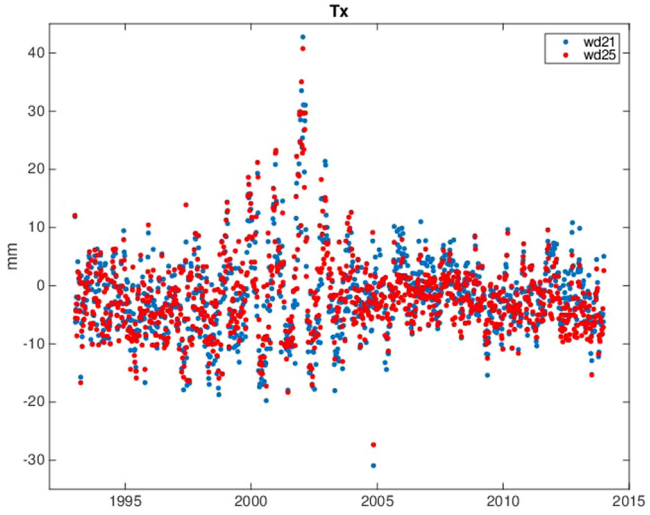

Fig. 3. Helmert transformation parameter Tx, for the gscwd21 and gscwd25 SINEX series to illustrate the impact of the use of the 5×5 time-variable gravity time series.

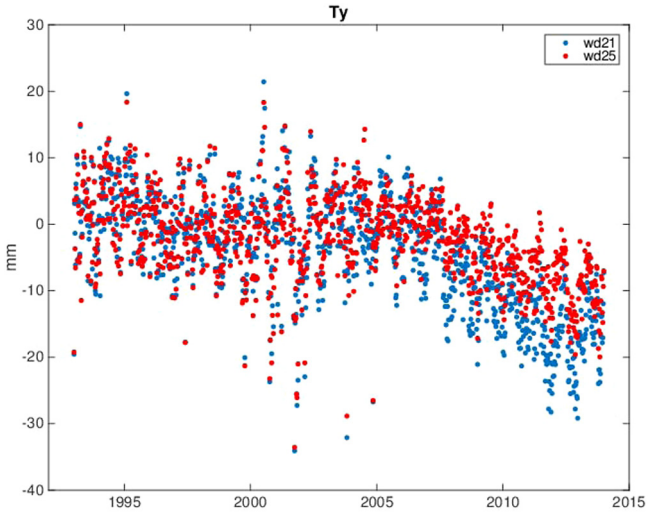

Fig. 4. Helmert transformation parameter Ty, for the gscwd21 and gscwd25 SINEX series to illustrate the impact of the use of the 5×5 time-variable gravity time series.

In Figs. 3 and 4, we illustrate the Helmert parameters for the gscwd21 and gscwd25 series to illustrate the impact that more detailed modeling of the time-variable gravity has on the recovery of the station coordinate time series. All available DORIS stations are used with equal weight in an unconstrained least-squares estimate of the seven Helmert parameters (3 translation, 1 scale, 3 rotation) for transformation of the weekly solution coordinates to the

Table 6
Summary of Helmert transformation parameters for the SINEX series, gscwd21, gscwd23 and gscwd25, illustrating impact of more detailed modeling of time-variable gravity.

Series	Time Span	Tx			Ty		
		Std (σ) mm	Annual Ampl. mm	Slope mm/y	Std. (σ) mm	Annual Ampl. mm	Slope mm/y
21	1999.0–2004.0	8.49	5.83	0.210	6.73	4.02	−0.316
23	1999.0–2004.0	7.42	4.72	0.386	6.01	3.17	−0.280
25	1999.0–2004.0	8.24	5.06	0.415	6.66	4.02	−0.258
21	2005.0–2014.0	4.78	2.78	−0.367	8.13	4.10	−2.351
23	2005.0–2014.0	3.86	1.83	−0.415	5.63	2.90	−1.528
25	2005.0–2014.0	3.96	1.70	−0.430	5.54	2.74	−1.505

DPOD2008 frame (Willis et al., 2015). [The estimated rotation values are very small indicating, as desired, no net rotations with respect to DPOD2008]. The Helmert parameters are shown in Table 6. Comparing gscwd23 and gscwd25 to gscwd21 shows the impact of improved time-variable gravity modeling on the reference frame translation parameters, Tx, and Ty. For the period 2005–2014, the more detailed TVG modeling reduces the standard deviations in Tx and Ty, reduces the amplitude of the annual terms in Tx and Ty, and also reduces the drift in Ty. An explanation for this improvement is provided by Rudenko et al. (2014) and by Couhert et al. (2015) who observe that the changes in the time-variable gravity field if not modeled in sufficient detail can induce radial orbit drifts that have largely a degree/order 2 character (Couhert et al., 2015, see Fig. 4).

One characteristic of the GSC SINEX DORIS series is high annual amplitudes in Tx from 1998 to approximately 2003. The more detailed time-variable gravity modeling does not mitigate this behavior. Thus we conclude, that these larger amplitudes, especially for Tx, are an artifact of the measurement or force mismodeling on the lower altitude satellites (i.e SPOT-2 and SPOT-4) around the maximum of solar cycle 23.

4. Measurement model changes

For the DORIS processing at NASA GSFC related to ITRF2014, the three most important measurement model related changes were (1) the modification of GEODYN to allow for deviations from the nominal frequency at the DORIS stations; (2) the implementation of the modeling of antenna phase center variations for the Starec and Alcatel antennae; and (3) direct computation of the antenna offset corrections in GEODYN rather than using the DORIS-data supplied offset corrections, as for ITRF2008 (Le Bail et al., 2010).

4.1. Beacon frequency corrections

Prior to 2002, the DORIS data delivered to the IDS data centers were corrected for deviations from the nominal beacon frequency. After 2002, all data had to be corrected by the data analysts to allow for the beacon frequency deviations. In GEODYN, this potential beacon frequency change was accommodated by modifying the partial derivatives for the estimation of the range-rate bias, and the applied bias. In GEODYN, we process DORIS data as a one-way ground-to-satellite range-rate measurement, and estimate a range-rate bias per pass to accomodate the offsets in frequency between the DORIS ultrastable oscillator on the satellite, and the frequency of the DORIS transmitter at the stations. GEODYN did not account for these beacon frequency deviations from the nominal value in the DORIS processing for ITRF2008.

In order to validate the changes, we tested the implementation on Jason-2 DORIS-only orbits for cycles 1–128 (July 12, 2008 to January 2, 2012). As in Moreaux et al. (2016), we estimated the Yarragadee coordinates using the Jason-2 data, and verified that the discontinuities in the statin height were removed. Regarding the POD performance, we find the RMS of fit is improved w.r.t. the mean, from 0.3772 to 0.3756 mm/s, and w.r.t. the median, from 0.3763 to 0.3745 mm/s. There is a demonstrable improvement in the DORIS RMS of fit per arc over nearly

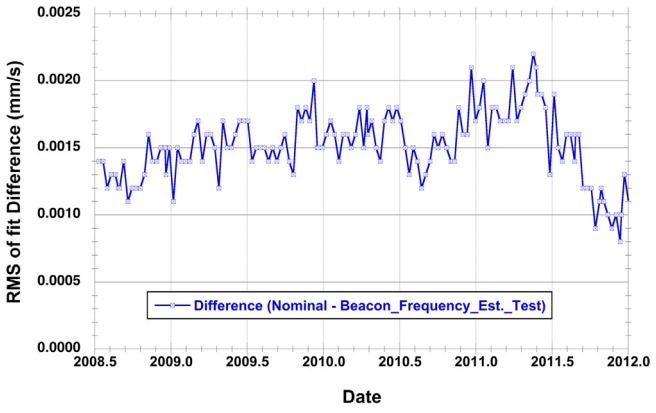

Fig. 5. Difference in Jason-2 RMS of fit for DORIS-only near-ten-day arcs from cycle 1 to 128 (July 12, 2008 to January 2, 2012), between a baseline run with and without the beacon frequency correction. A positive difference indicates an improvement in the DORIS RMS of fit when the estimation of the change from the nominal DORIS beacon frequency is applied.

the entire time span (see Fig. 5). We also analyzed the change in the DORIS RMS of fit on a station-by-station basis. We see an improvement, albeit small, for three-quarters of the DORIS stations. The improvement in RMS of fit is pronounced (larger than 0.006 mm/s) for the following stations: Arequipa (ARFB); Syowa (SYPB); Yarragadee (YASB); Rio Grande (RIQB & RIRB), and Tristan da Cunha (TRIB). We note a slight degradation in the RMS of fit (0.001–0.002 mm/s) for four stations: Santiagio (SANB); St. Helena (HEMB); Ascension Island (ASEB); and Libreville (LICB). It is a curious coincidence that these four stations were among those most affected by the South-Atlantic-Anomaly-induced perturbations on the SPOT-5 DORIS oscillator. It is possible the position and velocity of these stations in ITRF2008 (and consequently DPOD2008) were slightly degraded by the impact of the SAA on the SPOT-5 DORIS oscillator (Štěpánek et al., 2013), even though it was only one of the four to five members of the DORIS satellite constellation from 2002 to 2008. An alternative explanation could be that the Ultra Stable Oscillator (USO) on Jason-2 also has experienced the effects of perturbations due to the South Atlantic Anomaly, albeit at a lower level than Jason-1 or SPOT-5, (Pascal Willis, Institut national de l'information géographique et forestière & Institut de Physique du Globe de Paris, Paris, France, personal communication, October 2015). Belli et al. (2015) characterized the behavior of the DORIS USO using the Jason-2 T2L2 experiment and they present data (cf. Figs. 2 and 3 in their paper) that also suggest that this is a possibility.

After the validation with Jason-2, we then generated a complete SINEX series (gscwd18, 1992 to 2013.0, see Table 1) that applied the beacon frequency correction to compare with the antecedent time series without the correction (gscwd17, see Table 1). In Fig. 6 we show the scale w.r.t. DPOD2008 for the two series, as well as the difference in the DORIS scales. As expected, except for some minor estimation noise, the change in scale is close to zero prior to 2002. From 2002.0 to 2013.0, the mean change in scale is 4.2 mm, although occasional individual differences can reach 15 mm. Most importantly, a spurious long-term signature in the DORIS scale is removed. As shown in Table 7, the WRMS is reduced from 11.59 to 10.05 mm. Although the Tz for DORIS data is noisy compared to the other geodetic techniques, the correct beacon frequency estimation also reduces the standard deviation in the Tz parameters from 20.54 mm to 17.14 mm.

4.2. Phase Law Implementation and the impact of GEODYN-computed antenna offset corrections

We tested the implementation of the correction for antenna phase center variations of the DORIS antennae using TOPEX, Jason-2, SPOT-2 to SPOT-5, and Envisat. The form of the phase center variations for DORIS is described by Tourain et al. (2016), and is available from ftp://ftp.ids-doris.org/pub/ids/stations/doris_phase_law_antex_starec.txt. The Alcatel phase law varies within ±5 mm over the entire range of elevation angles. The Starec antenna phase law is bounded by ±5 mm, but only above about 25° elevation. Between 10° and 20° elevation

Table 7
Statistics of the gscwd17 and the gscwd18 SINEX series, to illustrate the impact of the estimation of changes from the nominal frequency for the DORIS stations on the Helmert transformation parameters for these SINEX series. The statistics are computed for 574 weekly arcs from 2002.0 to 2013.0. The units for the statistics of the Helmert parameters are in mm.

Parameter	gscwd17	gscwd18
WRMS (mean)	11.59 ± 2.06	10.05 ± 1.62
Tx (mean)	−2.43 ± 6.75	−1.67 ± 6.62
Ty (mean)	−4.88 ± 8.61	−5.74 ± 8.04
Tz (mean)	−6.75 ± 20.54	−11.07 ± 17.14
Scale (mean)	−1.68 ± 3.58	2.50 ± 2.92

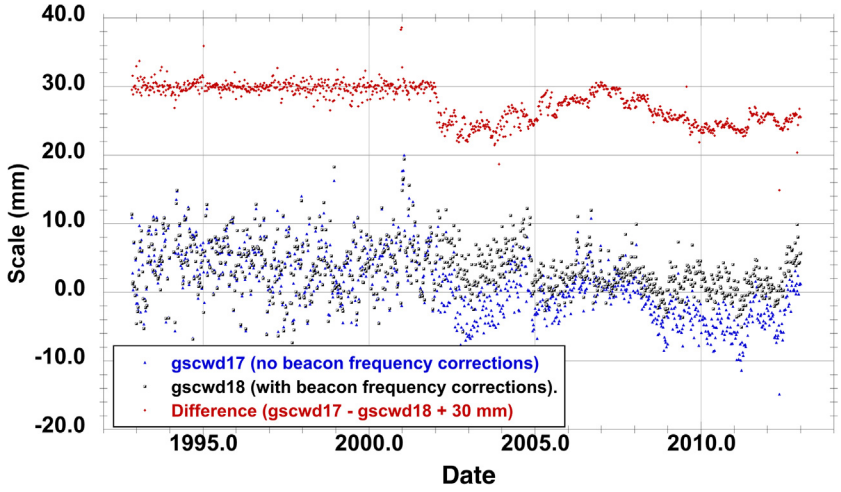

Fig. 6. Scale with respect to DPOD2008 for the gscwd17 SINEX series (no beacon frequency correction) and gscwd18 (includes the beacon frequency correction). The difference in scale between the two SINEX series (gscwd17 - gscwd18) is also shown and is translated +30 mm for clarity.

the phase law correction ranges from 7 to 13 mm. Since the NASA GSFC DORIS processing for ITRF2008 through SINEX series gscwd20 (see Table 2) used the data-supplied tracking point corrections, we had to first test the application of the antenna offset corrections on a satellite-by-satellite basis, and then in a second step test the application of the phase law. The validation of the calculation of the antenna offset correction tested both the knowledge of the satellite attitude, as well as the validity of the antenna offset coordinates for the DORIS 2 GHz phase centers, together with the knowledge of the center of mass in the spacecraft coordinate system.

In order to model the satellite attitude for Cryosat-2, we used the quaternions supplied by T.U. Delft (http://ids-doris.org/data-products/tables-of-data-products.html) for the SINEX series gscwd21 to gscwd25, and for the gscwd26 SINEX series, we used the internal attitude model in GEODYN derived from Cerri and Ferrage (2013).

4.2.1. TOPEX and Jason-2

In the case of TOPEX and Jason-2, we have had abundant experience with POD for these altimeter satellites (e.g., Marshall et al., 1995; Lemoine et al., 2010; Cerri et al., 2010). For DORIS-only orbits, we have independent data in the form of satellite laser ranging (SLR) data and altimeter crossovers. The modeling has always included direct modeling of the antenna offset corrections, which in some cases were empirically adjusted (Marshall et al., 1995). TOPEX follows a well-prescribed attitude law. For off-nominal arcs, we apply quaternions to model the TOPEX satellite attitude. We used spacecraft attitude information in the form of quaternions for only ~5% of the TOPEX arcs (36 out of a total of 679 data arcs). In the case of Jason-2, we already applied the quaternions to model the satellite attitude in the force model, so herein we also used them in the measurement model. We first looked at the aggregate results, which are summarized in Table 8. The TOPEX tests were conducted over three years from January 10, 1993 to January 15, 1996. The Jason-2 tests were conducted over four years from July 12, 2008 to July 27, 2012. For the TOPEX tests, 81 percent or 43 of the stations were Alcatel, while 19 percent or 10 of the stations were Starec. The Jason-2 tests involved 68 separate stations, all equipped with the Starec antenna. The Jason-2 tests show unambiguously that the CNES-derived Starec antenna phase law, on average improves the DORIS residuals, and also slightly improves the SLR and altimeter crossover residuals. For TOPEX we show an overall reduction in the DORIS residuals from 0.5320 mm/s to 0.5311 mm/s, and a small (0.01 mm) reduction in the altimeter crossover residuals. The reduction in the DORIS residuals applies to both the Alcatel antennae (0.5285–0.5260 mm/s) and the Starec antennae (0.5328–0.5322 mm/s). We also computed the orbit differences due to application of the phase law. For TOPEX, the average RMS orbit differences over 110 cycles were 0.3 mm radial, 2.6 mm cross-track and 1.0 mm along-track. For Jason-2, the average RMS orbit differences were 0.5 mm radial, 6.2 mm cross-track, and 1.3 mm along-track.

Table 8
TOPEX/Poseidon and Jason-2 precise orbit determination summary. The Jason-2 tests are conducted over Jason-2 cycles 1–112 (July 12, 2008 to July 27, 2012). The TOPEX/Poseidon (TP) tests are conducted over TP cycles 12–122 (January 10, 1993 to January 15, 1996).

Test	DORIS (mm/s)	Independent data	
		SLR (cm)	Altimeter crossovers (cm)
	TOPEX/Poseidon		
no phase law	0.5320	4.651	5.857
include phase law	0.5311	4.661	5.856
	Jason-2		
no phase law	0.3748	1.815	5.480
include phase law	0.3745	1.810	5.478

We then aggregated the DORIS residuals across all the arcs for TOPEX and Jason-2, and computed per 1° bin, the change in the RMS of the residuals due to the application of the phase laws. We show this for Jason-2 in Fig. 7. The peak in the RMS residual differences between 65° and 72° is responsible for about 65% of the variance reduction due to the application of the phase law. In Fig. 8 we show these differences in RMS of fit binned by elevation for both the Alcatel and Starec antennae as seen in the TOPEX tests. For the Alcatel stations as seen by TOPEX, the residuals are notably worse between 68° and 75° elevation, but show a marked improvement at the higher elevations (above 76°). The Alcatel phase law was supplied by the manufacturer, and as of this writing, no anaechoic measurements have been made to confirm this information (Tourain et al., 2016). We cannot say from these results alone whether this mixed performance can be ascribed to the erroneous Alcatel phase law at those elevations (68–76°) without confirmation of similiar behavior on other DORIS satellites (such as SPOT-2 and SPOT-3).

4.2.2. SPOT satellites

For other satellites, especially the SPOT satellites, we do not have explicit information as to how well they followed their respective attitude laws, as described in Cerri and Ferrage (2013). We performed the two tests described above in 1995 for SPOT-2 and SPOT-3, and in 2011 for SPOT-4 and SPOT-5. In Fig. 9 we show the difference in RMS of fit for two tests: (1) where the antenna offset corrections were computed in GEODYN using the prescribed SPOT satellite phase law (Cerri and Ferrage, 2013), and (2) where in addition the DORIS antenna phase laws for the Alcatel and Starec antennae were applied. In this way we can assess the application of the satellite attitude law in combination with the antenna offset information that has been supplied for these spacecraft. For SPOT-2, we see a systematic improvement (average of 0.002 mm/s) when the GEODYN-computed corrections are applied. This systematic improvement may imply that the antenna offsets, center of mass or attitude law now available are superior to

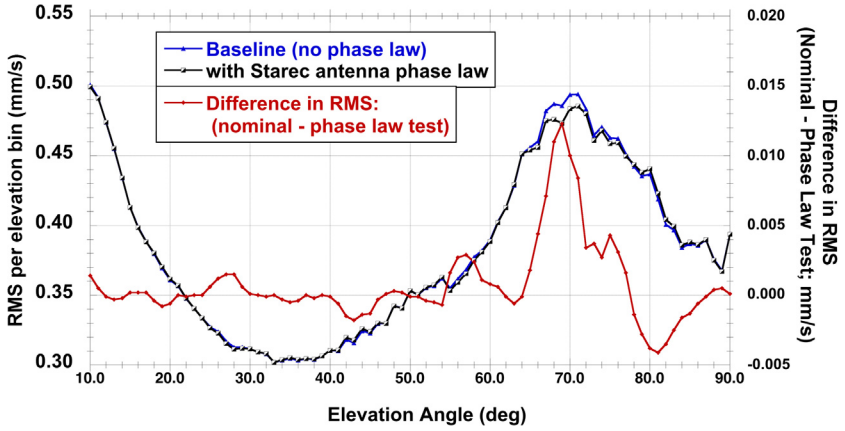

Fig. 7. RMS DORIS residuals vs. elevation for Jason-2 cycles 1–112 (July 12, 2008 to July 27, 2012) for the baseline case (no phase law applied), and for the test case (applying the phase law), as well as in red, the difference in the RMS per elevation bin. The sense of the difference is "baseline - test", such that a positive difference shows an improvement in the DORIS RMS of fit due to application of the phase law. These tests with Jason-2 concern only the Starec antennae.

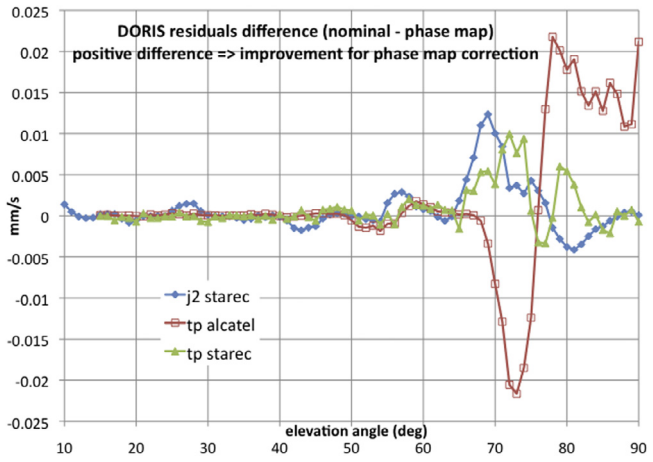

Fig. 8. RMS DORIS residuals vs. elevation for TOPEX cycles 12–122 (January 10, 1993 to January 15, 1996) for the baseline case (no phase law applied), and for the test case (applying the phase law), as well as the differences in the RMS binned residuals, shown separately for the Alcatel and Starec antennae.

what was used to compute the original corrections on the SPOT-2 data. For SPOT-3, the application of the GEODYN-computed antenna offset corrections does not, on average, change the RMS of fit, however the application of the DORIS antenna phase law demonstrably improves the RMS of fit by an average of 0.0050 mm/s. For SPOT-4 and SPOT-5 we observe that for a period of approximately two months, the application of the nominal attitude law and the GEODYN-computed attitude corrections actually degrades the RMS of fit. We conclude that for these two months, the satellites were not following the nominal phase law described by Cerri and Ferrage (2013). The dates correspond to 2011-04-10 to 2011-06-26 for SPOT-4, and 2011-03-27 to 2011-06-05 for SPOT-5. The dates for SPOT-5 are close to but do not coincide completely with the dates of one of the step changes in the scale of SPOT-5 single-satellite SINEX solutions (Moreaux et al., 2016, see Fig. 9).

4.2.3. Envisat

We also tested Envisat DORIS data in two periods: (1) 2011, and (2) 2002.4 to 2006.0. For Envisat in 2011, we see an improvement for both the use of the GEODYN-computed tracking point offsets, and a smaller improvement for the application of the phase law. The average improvement in the RMS of fit from the antenna offset corrections is 7.39×10^{-3} mm/s, and the average improvement in the RMS of fit due to the application of the phase law is 1.19×10^{-3} mm/s.

In developing the gscwd21 SINEX series (see Table 2), we evaluated the RMS of fit for Envisat in applying both the antenna offset correction and the antenna phase laws. We found that between the start of the Envisat mission in 2002 and 2005.0, the average improvement in RMS of fit was 0.0369 mm/s, compared to an improvement of only 0.00119 mm/s for 2005 (see Fig. 10). We hypothesize that the DORIS-data-supplied corrections in 2003 and 2004 on Envisat are at least partially erroneous and this explains the large improvement we see in the DORIS RMS of fit. We have verified that the improvement we see is not due to any change in the number of observations per arc that might occur due to dynamic data editing.

4.2.4. Impact on scale

Having validated the mechanics of the implementation of the phase law, and the computation of the antenna offset corrections in GEODYN, we then computed a SINEX series (gscwd21, see Table 2). In Fig. 11 we show the impact of the application of the DORIS phase law on the scale of the DORIS coordinate solutions. The primary effect of applying the phase law is a shift in the scale of +5.99 mm from 1993/01/03 to 2002/06/06 (prior to the inclusion of Envisat and SPOT-5), and by +10.67 mm from 2002/06/13 to 2008/07/06, +12.27 mm from 2008/07/13 to 2010/05/30 (due to the inclusion of Jason-2) (see Table 9). The change in scale is smaller when the network is dominated by the Alcatel antennae, and larger when the network is dominated with the Starec antenna (Moreaux et al., 2016). In

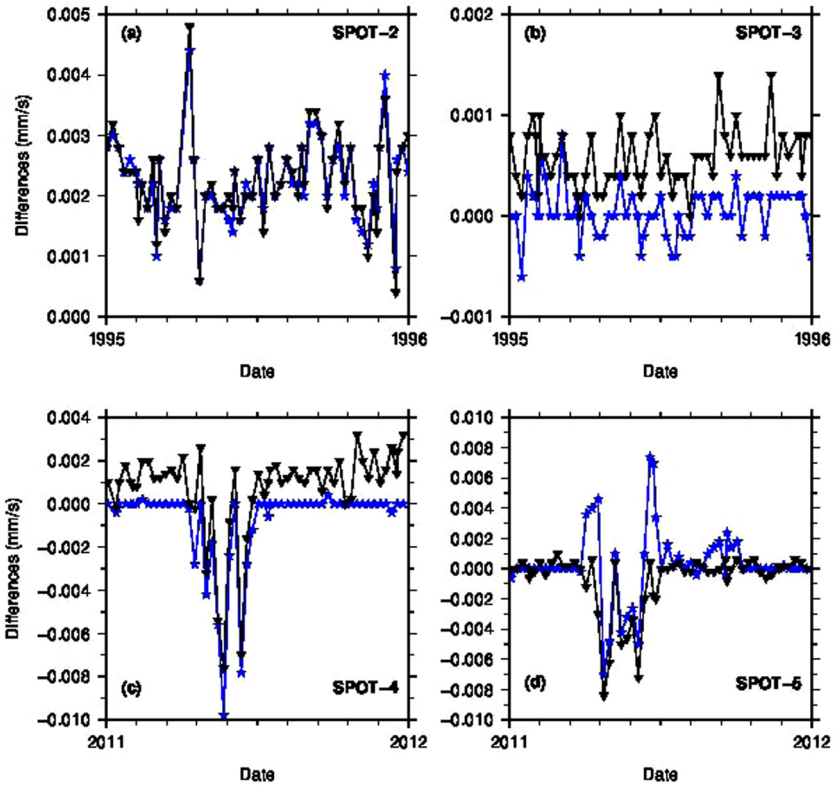

Fig. 9. SPOT Satellites: Test of GEODYN-computed antenna offset corrections (blue curves, asterisk symbols) and GEODYN-computed antenna offset corrections + phase law (black curves, triangle symbols) on (a) SPOT-2, and (b) SPOT-3 in 1995, and (c) SPOT-4, and, (d) SPOT-5 in 2011. The tests are shown as differences with respect to the same data arcs computed without these corrections, and that used the DORIS-data-supplied (format2.2) antenna offset corrections. A positive value indicates an improvement for the respective test. (For interpretation of the references to color in this figure legend, the reader is referred to the web version of this article.)

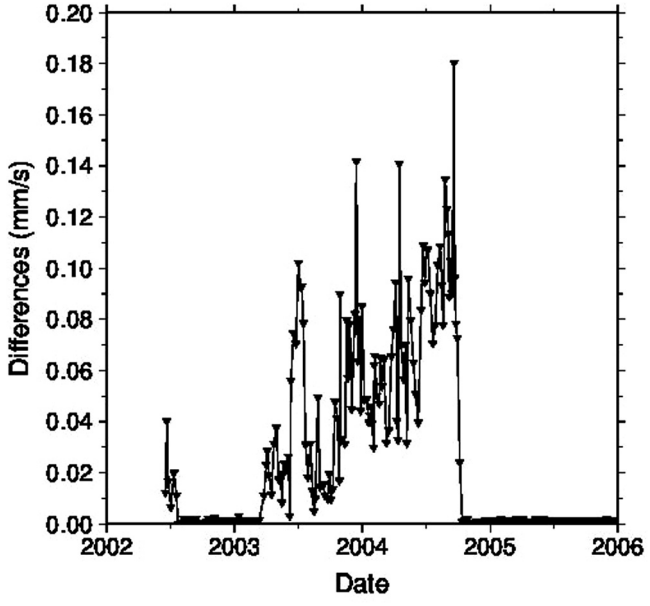

Fig. 10. Envisat (2002.4–2006.0): Improvement in RMS of fit for Envisat with the gscwd21 SINEX series compared to the gscwd20 SINEX series (see Table 2). The changes reflect the application of the GEODYN-computed antenna offset corrections and the DORIS antenna phase law. The average improvement from 2002 to 2005.0 is 0.0369 mm/s; the average improvement in RMS of fit is 0.00128 mm/s for 2005.

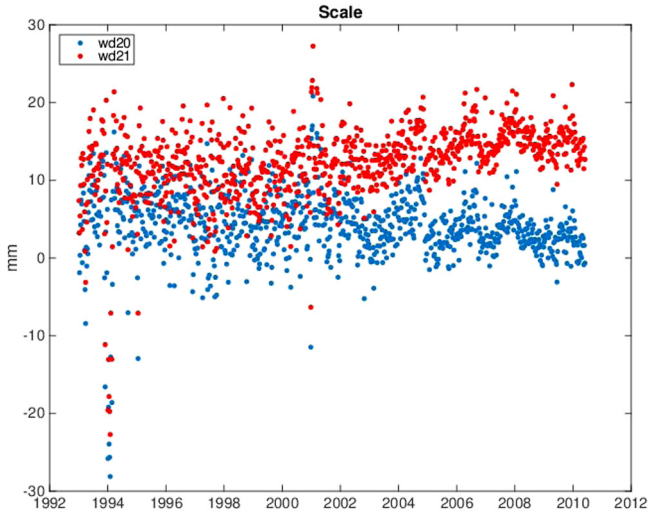

Fig. 11. Scale of the gscwd20 and gscwd21 solutions wrt. DPOD2008. The gscwd21 SINEX series applies the DORIS tracking coordinate offsets in the GEODYN orbit determination software, and applies the DORIS antenna phase laws (Tourain et al., 2016). We only show the comparisons of the two SINEX series from January 3, 1993 through the week of May 30, 2010, prior to the incorporation of Cryosat-2 into the DORIS solutions.

Table 9
Statistics of the gscwd20 and the gscwd21 SINEX series, to illustrate the impact of applying the GEODYN-computed DORIS antenna offset corrections, as well as the DORIS antenna phase laws for the Alcatel and Starec antennae (Tourain et al., 2016). The statistics are computed for the weeks of January 1, 1993 to October 30, 2011, before the introduction of HY-2A. We only show the WRMS, Tz and the scale since Tx, and Ty change negligibly. The units for the statistics of the Helmert parameters are in mm.

Dates	1993/01/03 to 2011/10/30		1993/01/03 to 2002/06/06		2002/06/13 to 2008/07/06		2008/07/13 to 2010/05/30	
Comments	No HY-2A				Add Envisat & SPOT-5		Add Jason-2	
Series	wd20	wd21	wd20	wd21	wd20	wd21	wd20	wd21
No. of weeks	983		493		317		99	
WRMS								
(mean)	12.31	12.28	14.82	14.84	9.86	9.74	9.61	9.69
(median)	11.82	11.86	14.51	14.52	9.68	9.59	9.45	9.52
Tz (mean)	−6.58	−6.01	−2.77	−0.67	−11.28	−10.79	−6.28	−7.87
Tz (σ)	16.44	16.40	16.67	16.26	15.93	14.41	15.07	16.10
Scale (mean)	4.14	12.91	4.81	10.71	3.91	14.15	2.17	14.71
Scale (median)	3.98	13.20	5.36	11.35	3.61	14.28	2.35	14.62
Scale (σ)	4.30	4.98	5.42	5.43	2.78	2.76	1.90	2.05

addition to the change in the scale, the introduction of the phase law causes a shift in the Tz which is more pronounced in the latter part of the time series (after 2002) than in the early part of the time series. Table 9 also shows that notwithstanding the systematic signals remaining in the scale of the DORIS solutions, the precision of the scale has improved from 5 mm in standard deviation before 2002, to 2 mm after the introduction of the DGXX DORIS data from Jason-2.

5. Data processing

5.1. DORIS time bias

As noted in Zelensky et al. (2006) for joint SLR and DORIS orbit determination, we routinely adjust a time bias for the DORIS measurements over the arc. This represents the bias in the DORIS time system, with respect to the time system of the SLR tracking stations. For TOPEX, the time biases approached −28 μsecs in December 1994, but later in the mission we find the time biases to be no more than ±5 μsec. In order to mitigate the along-track orbit error that might deleteriously affect the satellite positioning, we implemented a model of the DORIS time bias variations for the DORIS-only processing on TOPEX, represented as a piece-wise continuous line in Fig. 12.

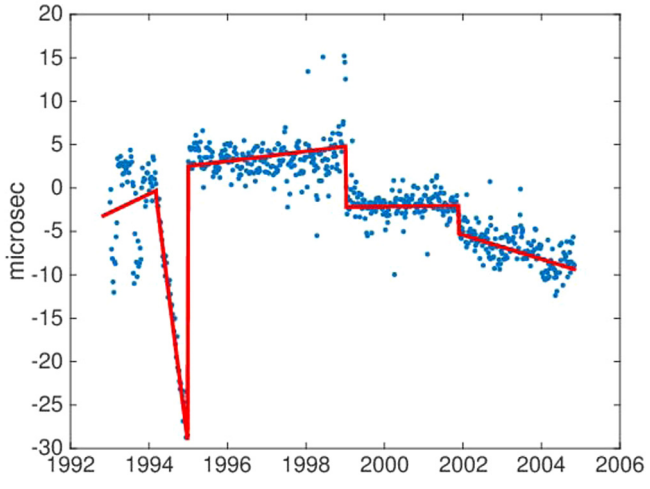

Fig. 12. DORIS time bias derived from SLR and DORIS solutions for TOPEX using the final ITRF2014 (gscwd25) processing standards. The time bias for TOPEX reaches −28 μsecs in December 1994 (blue dots). A simplified DORIS time bias model (shown as a piecewise continuous red line) derived from earlier processing was applied in the derivation of the gscwd25 and gscd26 SINEX series. (For interpretation of the references to color in this figure legend, the reader is referred to the web version of this article.)

We evaluated the impact of applying this time bias by computing an independent SINEX series (gscwd22a, see Table 2) from 1993 to 2004, the span of the TOPEX mission. From January 1993 to November 2004, the WRMS is reduced from 14.01 to 13.83 mm, so overall we see a small net improvement. Modeling the DORIS time bias has an intriguing impact on the Helmert parameters of the combined solution. The most interesting effects are in Ty and the scale, where we see annual signals in the differences of gscwd22a with the baseline series for this test, gscwd20. The annual signal in the Ty differences is ±5 mm, whereas in scale the annual signal reaches ±2 mm between 1994 and 1996, when the DORIS time bias are largest in amplitude. The Tx differences are largest (±5 mm) between 2000 and 2003, near the peak of solar cycle 23. The average, median and standard deviation of the differences between the two time series are shown in Table 10.

Table 10
Differences in Helmert parameters between the gscwd20 and gscwd22a SINEX series, illustrating the impact on the weekly combination of modeling the TOPEX DORIS time biases. The sense of the differences are gscwd22a (with the time bias) – gscwd20 (without the time bias) and the units are in mm.

Parameter	Mean	Median (mm)	σ
Tx	0.86	0.81	2.84
Ty	0.12	0.00	3.62
Tz	0.61	0.64	3.22
Scale	0.09	0.52	0.09

We also evaluated the DORIS time biases on the other satellites that also had SLR tracking. We summarize in Table 11 the mean, median, and standard deviation of the DORIS time biases from joint processing with SLR data. Zelensky et al. (2006) reported an Envisat DORIS time bias of -7.1 ± 1.2 μsec, and Le Bail et al., 2010 found time bias values of 5–10 μsecs in absolute value. With the new Envisat data issued by the CNES (see DORISMAIL 0823, May 16, 2012, http://ids-doris.org/), we find that on average the Envisat DORIS time biases are less than 1 μsecs in absolute value. Similarly, the DORIS time biases computed for Cryosat-2 are also less than 1 μsec. However, Jason-1 has a mean DORIS time biases of -3.5 ± 1.3 μsecs, corresponding to 2.1 cm of potential systematic along-track error.

5.2. Processing of SAA-corrected data

The final SINEX series (gscwd26) used DORIS data for Jason-1 and SPOT-5 that were corrected for the perturbations caused by the South Atlantic Anomaly (SAA) on the DORIS satellite Ultra-stable oscillators (Lemoine and Capdeville, 2006; Štěpánek et al., 2013; Capdeville et al., 2016). We tested the SAA processing strategy by focusing on data in 2011. For Jason-1 we tested two strategies: (1) *SAA-Test1*: the DORIS stations most affected by the SAA were not downweighted in the precise orbit determination; (2) *SAA-Test2*: the Jason-1 arcs were computed with arcs that downweighted 29 designated SAA stations, following the strategy employed by Lemoine et al. (2010). For SPOT-5, there was no special treatment of the SAA stations (they were not downweighted). The SAA-related stations were not allowed to contribute to the general multi-satellite combination. We evaluated the impact on the RMS of fit, the WRMS and the Helmert parameters for the single-satellite and the combination solutions.

5.2.1. SPOT-5 SAA tests

In Fig. 13 we illustrate the impact of using the SAA-corrected data on the RMS of fit for SPOT-5. For the four stations in the vicinity of the SAA (CADB, ARFB, SANB, KRUB) the improvements are substantial. For Cacheoira, the station most affected, the RMS of fit is improved from 0.657 to 0.548 mm/s. Overall the RMS of fit is improved for all four stations from 0.434 to 0.429 mm/s. YASB (Yarragadee) and GREB (Greenbelt) are shown as "control points" since they are far from the SAA region. HEMB (St. Helena) is a station whose data is perturbed by the SAA for Jason-1, but we show for SPOT-5 that these data appear unaffected. We show the impact on the WRMS and the Helmert parameters in Fig. 14. Over the test period of 2011, the WRMS improves from 12.63 to 11.53 mm. The scatter (standard deviations) in Tx, Ty and Tz are slightly degraded (by up to 0.5 mm for Tz). Using the SPOT-5 SAA data shifts the mean Tz by 2.7 mm.

Table 11
DORIS time biases by satellite derived from joint processing the SLR data using the final (gscwd25) processing standards. The average, median and standard divation about the mean are shown in units of μsecs.

Satellite	Dates	Average	σ (μsecs)	Median
Cryosat-2	2010.4–2015.0	−0.26	1.65	−0.25
Envisat	2002.5–2007.0	−0.90	1.79	−1.22
Envisat	2007.0–2012.2	−0.50	1.27	−0.54
HY-2A	2011.8–2015.0	−1.63	1.55	−1.77
Jason-1	2004.9–2008.5	−3.45	1.25	−3.61
Jason-2	2008.5–2015.0	−1.19	1.03	−1.15
TOPEX	1992.9–1995.0	−6.66	9.21	−5.04
TOPEX	1995.0–1998.0	3.21	1.47	3.25
TOPEX	1998.0–2004.8	−3.34	4.51	−2.91

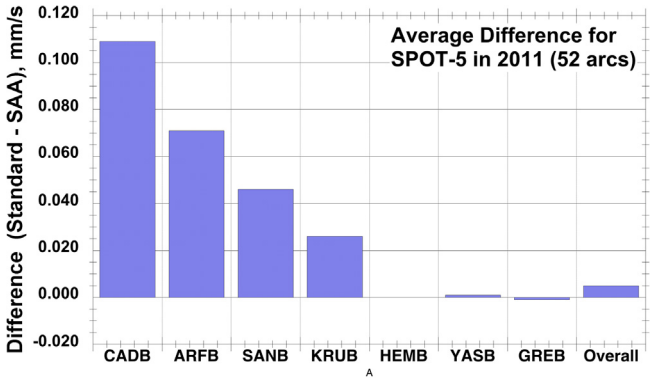

Fig. 13. Average change in the RMS of fit for 52 SPOT-5 data arcs in 2011. The differences illustrate the degree of improvement due to the use of the SPOT-5 SAA model (Štěpánek et al., 2013; Capdeville et al., 2016). The sense of the differences are "standard processing (non-SAA-corrected) – SAA-corrected", so a positive change indicates an improvement.

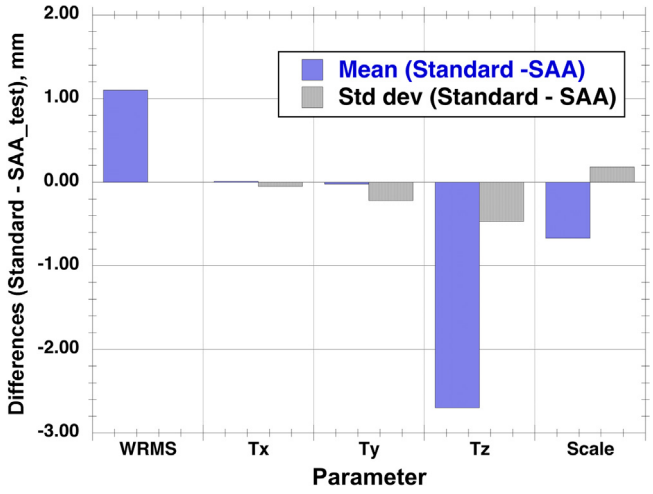

Fig. 14. Change in the mean WRMS, and change in the mean and standard deviation of the Helmert parameters, from comparing two SINEX solutions in 2011 that process the standard SPOT-5 DORIS data, and the SAA-corrected DORIS data for SPOT-5. The baseline SINEX solution is gscwd15 (See Table 2). The sense of the differences are "standard - SAA test". A positive change in this figure for the delta in the standard deviations indicates an improvement due to the use of the SAA-corrected data.

5.2.2. SAA tests on Jason-1

We have previously found that in order to obtain good orbit determination performance and prevent an excessive Z-shift in the orbit, it is necessary to downweight the SAA-related stations on Jason-1 (e.g., see Lemoine et al., 2010). Over 2011, the overall DORIS RMS of fit for *SAA-Test1* (no downweighting) is 0.427 mm/s, for *SAA-Test2* (with downweight of up to 2.67 for some SAA stations) the RMS of fit is 0.366 mm/s. The SLR fit improves for *SAA-Test2* to 1.23 cm compared to 1.35 cm for *SAA-Test1*. For the test period in 2011, adding in Jason-1 to the baseline weekly combination (gscwd15) degrades the WRMS to 13.01 mm (*SAA-test1*), but improves it in the second case to 11.28 mm (*SAA-test2*). Thus downweighting the SAA stations in the orbit determination, as well as reducing the Jason-1 SAA stations (not allowing them to contribute to the combination) seems to be the preferred method of handling Jason-1. The addition of Jason-1 causes a shift in the DORIS scale of 4.6 mm, and a shift in the Tz Helmert parameter of 2 mm (see Fig. 15). This test shows that the addition of Jason-1 can benefit a weekly station coordinate solution, even when Jason-2 is present. For ITRF2014, we only added Jason-1 from November 2004 to July 2008. In light of these tests, the possible benefits of including Jason-1 over a longer period of time (after the launch of Jason-2) should also be assessed, although the impact on the DORIS scale will need to be carefully evaluated.

5.3. Parameterization of empirical accelerations

Previously in Le Bail et al. (2010), we adjusted the empirical accelerations along-track and cross-track to the orbit once per day over the each data arc. This parameterization was shown to quite effective in empirically removing

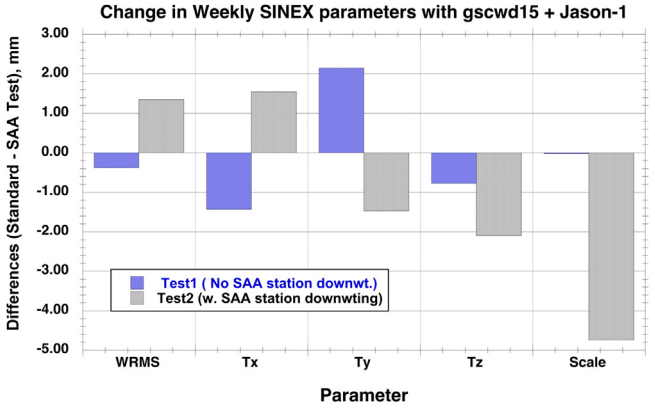

Fig. 15. Change in the mean WRMS, and change in the mean and standard deviation of the Helmert parameters, from comparing two SINEX solutions in 2011 that process the Jason-1 SAA data. The two tests compare two strategies for weighting of the SAA-related stations on Jason-1. In Test 1, no downweighting of any stations is applied; In Test 2, 29 stations are downweighted by up to 2.67, based on their proximity to the SAA region. The baseline SINEX solution for these comparisons is gscwd15 (See Table 2). The sense of the differences are "standard - SAA test", so for the WRMS, a positive change indicates an improvement.

residual force model error for satellites such as TOPEX, Jason-1, and Jason-2, when dynamic orbits (as opposed to reduced-dynamic orbits) were considered (e.g., see Marshall et al., 1995; Lemoine et al., 2010). However, in analyzing the empirical accelerations for the DORIS-only satellite precise orbit determination, it became apparent that the cross-track accelerations were more poorly determined than the along-track accelerations. Štěpánek et al. (2014) showed in their DORIS analysis that the adjustment of cross-track empirical accelerations weakened the determination of the estimated pole coordinates. For the gscwd26 SINEX series (see Table 2), we adjusted the along-track accelerations daily, while we adjusted the cross-track accelerations only once per orbital arc. Since most of the DORIS data arcs were seven days in length, this meant that we adjusted one cross-track acceleration once per seven days, most of the time.

We illustrate the overall impact of adjusting the cross-track accelerations less frequently in Fig. 16. Adjusting the cross-track accelerations less frequently on average reduces the amplitude and the scatter for all the DORIS satellites. The median amplitude is reduced by 55.22% for SPOT-3, 64.26% on SPOT-5, and 74.76% on TOPEX. We see the lowest reductions for the DGXX-equipped satellites: 10.70% for Jason-2, 9.35% for Cryosat-2, and 5.98% for HY-2A. The amplitude of the along-track accelerations changes negligibly between gscwd25 and gscwd26. These results imply that for DORIS-only satellite orbit determination, adjusting cross-track accelerations daily could weaken the determination of both the orbit and of the geophysical parameters.

If we examine the recovered cross-track accelerations, we find that for some satellites (e.g. SPOT-2 and SPOT-4), the accelerations determined daily have a completely random appearance, whereas those determined less frequently show a coherent annual signal. For both these satellites, we suppose radiation pressure mismodeling, with some contribution by incomplete modeling of atmospheric drag are responsible. As an example we showed the amplitude of the daily accelerations for SPOT-4 in Fig. 17. Improvements of the radiation pressure modeling, for example using the approach of Ziebart (2004), might be able to reduce the amplitude of these cross-track accelerations.

6. Results

We now summarize the results of our DORIS analysis for ITRF2014 by discussing the WRMS of the SINEX series (gscwd25 and gscwd26), the scale of the DORIS solutions, and the quality of the Earth Orientation Parameters (EOPs).

6.1. WRMS

In Table 12 we summarize the WRMS for the different SINEX series developed in the course of the work for

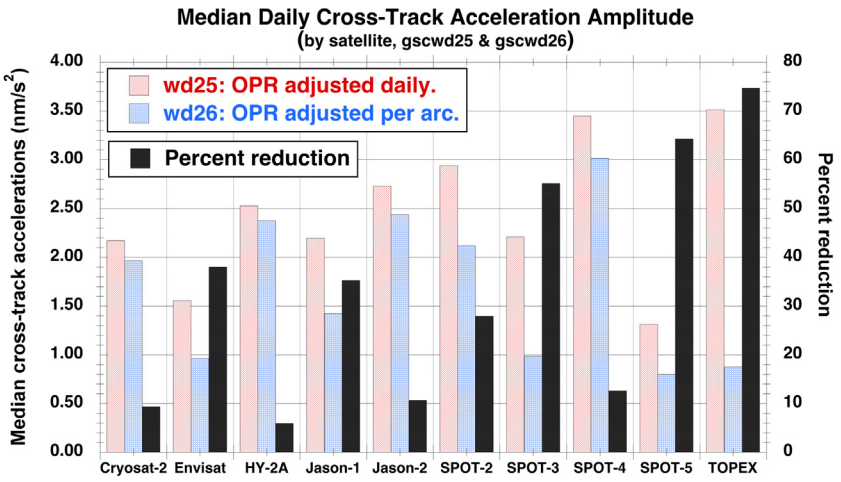

Fig. 16. Median cross-track acceleration amplitude by satellite for the gscwd25 and the gscwd26 SINEX series, as well as the percent reduction in the median accelerations for gscwd26, compared to gscwd25. The medians are computed all the available satellite arcs for each satellite and are in units of nanometers/s^2.

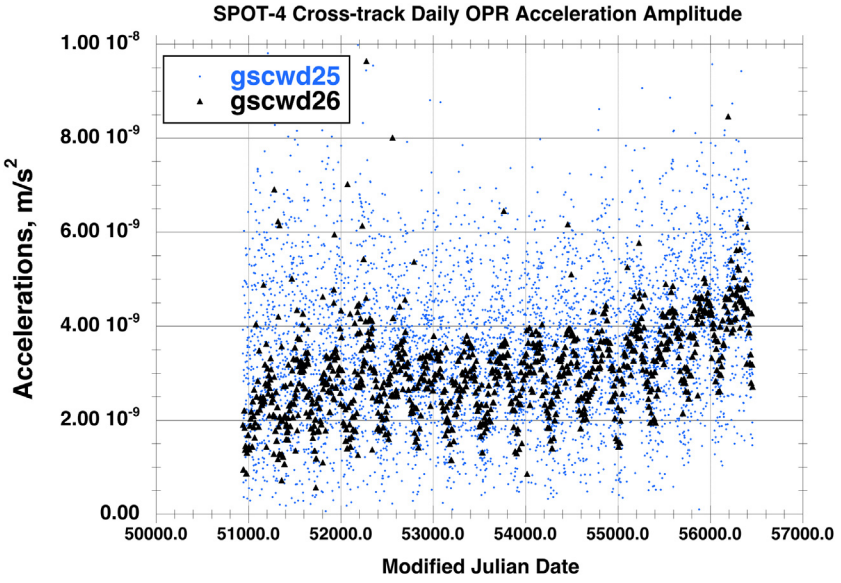

Fig. 17. Cross-track acceleration amplitudes for SPOT-4 from 1998 to 2013 for gscwd25 (adjusted daily) and gscwd26 (adjusted per arc, generally weekly). The mean, median, and RMS are 3.60, 3.45, and 4.18 nm/s^2 respectively for gscwd25, and 3.01, 3.01, 3.14 nm/s^2 respectively for gscwd26.

ITRF2014 (See Table 2 for a description of each series). Each series is compared to the WRMS reported for SINEX series gscwd10, delivered for ITRF2008 (Le Bail et al., 2010). We show the WRMS according to the data periods defined by the changes in the satellite constellation we used for ITRF2014. The final WRMS is 8.50 to 9.89 mm after the inclusion of data for Jason-2. The smallest improvements occur early in the mission, when data from only two or three satellites (TOPEX & SPOT-2 and SPOT-3 or SPOT-4) were available. From this table, we can quantify which set of changes had the most impact over a particular time period. From 1998/0503 to 2008/0706, the cumulative changes from Le Bail et al. (2010) result in an improvement inf WRMS of 16.08% to 24.11%. The time variable gravity generally provides a smaller improvement in the WRMS, 2.48% to 8.50%, except after 2012/0401 where the improvement is 20.56%. We note that in the SPOT-3 time frame, the time-variable gravity time series degrades the WRMS by 3.76%. This suggests perhaps that the impact of zero knowledge for the spacecraft center of mass for this satellite, and the inclusion of SPOT-3 in the time-variable gravity solutions should be reevaluated.

In Section 5.3, we showed that reducing the frequency of adjustment for the cross-track empirical accelerations had a profound effect on their amplitude and structure. Nonetheless, we see only a small improvement on the WRMS of 0.06% to 2.94%.

Table 12
WRMS for GSFC SINEX series developed for ITRF2014, compared to WRMS for the SINEX series developed for ITRF2008 (gscwd10) (Le Bail et al., 2010). For details of the series see Table 2. The WRMS for the ITRF2014 series are computed w.r.t. DPOD2008 (Willis et al., 2015); The WRMS for gscwd10 are as reported by Le Bail et al. (2010). The units are mm.

Dates	No of Satellites	SINEX series WRMS (mm)					
		ITRF2008	ITRF2014				
		wd10	wd15	wd20	wd21	wd25	wd26
930103–940130 (S2,TP)	2	17.33	17.37	16.88	16.91	16.91	16.92
940206–961110 (S2,S3,TP)	3	14.59	14.39	14.07	14.09	14.62	14.19
961117–980426 (S2,TP)	2	17.34	17.00	16.46	16.50	16.55	16.54
980503–020609 (S2,S4,TP)	3	16.79	14.57	14.26	14.21	14.09	14.08
020616–041031 (EN,S2,S4,S5,TP)	5	12.45	12.01	10.77	10.44	10.01	9.99
041107–080706 (EN,J2,S2,S4,S5)	5	11.20	9.82	9.27	9.29	8.50	8.50
080713–100530 (EN,J2,S2 S4,S5)	5	–	11.90	9.61	9.69	9.45	9.43
100606–111030 (C2,EN,J2,S5,S5)	5	–	12.24	9.67	9.66	9.16	9.11
111106–120325 (C2,EN,HY,J2,S4,S5)	6	–	13.27	10.06	10.68	9.95	9.73
120401–130609 (C2,HY,J2,S4,S5)	5	–	14.09	10.16	11.82	9.39	9.34
130616–141228 (C2,HY,J2,S5)	4	–	–	10.81	–	9.96	9.89

6.2. Scale

In Fig. 18, we show the scale for the series developed for ITRF2014, of which gscwd25 and gscwd26 were submitted as candidates for inclusion in the IDS combination (Moreaux et al., 2016). The figure shows the more stable scale compared to the series submitted for ITRF2008, which had a noticeable scale rate (Le Bail et al., 2010, See Fig. 9). We have eliminated the anomalous DORIS combination scales in early 1994 (visible in Fig. 18 for the scale of the gscwd20 SINEX series). The IDS AWG deduced that these were caused by spurious data on SPOT-2 (Moreaux et al., 2016). By using the artifice of adjusting a radial offset for SPOT-2 over the arcs from 1994/0102 to 1994/0220, we made the scale for those weeks to be more consistent with the solution scale over the adjacent weeks in 1993 and 1994. The mean SPOT-2 radial offset adjustment for these arcs was large, 6.63 ± 3.69 cm, and we infer that there is an intrinsic error in the data that is accommodated by this parameter adjustment.

As we have previously discussed, the implementation of the phase law shifts the scale by up to 12 mm after the inclusion of Jason-2, when the ground network includes only Starec antennae. Nonetheless, the gscwd20 and the gscwd26 SINEX series show the increase in scale in early 2012, that has been imputed to the Cryosat-2 and Jason-2 satellite (Moreaux et al., 2016), although with respect to these satellites and their DORIS data, no specific cause has been determined. As we discuss in the next section (Section 6.3), the HY-2A satellite has an offset of 30 mm in scale with respect to DPOD2008. Hence, when that satellite is added to our solutions starting in April 2012, this also

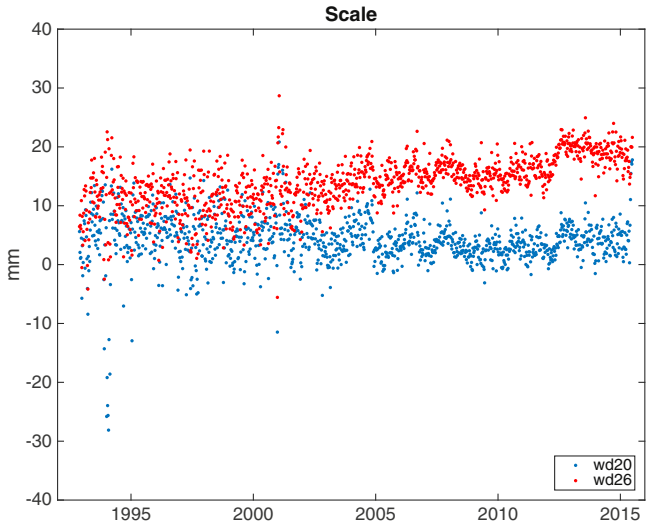

Fig. 18. Scale for the NASA GSFC DORIS SINEX series delivered for ITRF2014. The gscwd26 series was included in the IDS combination for ITRF2014 (Moreaux et al., 2016). The gscwd20 series used the DORIS-data-supplied antenna offset corrections, and applied neither the DORIS antenna phase law nor the improved modeling of time-variable gravity. The gscwd26 series applied the antenna phase law, applied an improved model of time-variable gravity, applied the ground & satellite antenna offset corrections in GEODYN, and included the HY-2A satellite after April 2012.

contributes to the increase in scale that is observed for the gscwd26 SINEX series. The mean and standard deviation of the scale for gscwd26 from 1993 to 2002/0609 (prior to the inclusion of Envisat and SPOT) is 11.19 ± 4.36; The mean and standard deviation of the scale for gscwd26 from 2002/0613 to 2010/1030 (prior to the inclusion of HY-2A) is 14.81 ± 2.18.

6.3. Single satellite solution scales

It is illuminating to compute the single-satellite SINEX solutions for the satellites that contributed to ITRF2014. We concentrate on the period after 2002, when five or more satellites contributed data. For each of the single-satellite solutions, we computed a solution in the same manner as for gscwd26, and then computed a station coordinate solution. We then estimated the Helmert parameters to transform the free-network solution to the reference solution, in this case DPOD2008. We show the results in Figs. 19 and 20. For the sake of clarity, we have smoothed the weekly solution scales with a five-week running average.

The scale of the single satellite coordinate solutions can reveal anomalies associated a particular satellite, that might pertain to an aspect of the DORIS data or the data corrections, or might reveal other issues with the spacecraft modeling. The first observation is that we see clearly the 'sawtooth' pattern in the scale of the SPOT-5-only solutions between 2002 and 2009, consistent with Moreaux et al. (2016). The SPOT-5 scale pattern imprints itself in the DORIS combination (for gscwd20, gscwd25, and gscwd26) as we see in Fig. 18. In addition, between 2011/0410 and 2011/0626 we see a local peak in the SPOT-5 scale. This peak coincides with the period of the anomalously high RMS of fit reported for SPOT-5 in Section 4.2.2. No explanation has been found for the 'sawtooth' pattern in the SPOT-5 scale (Guilhem Moreaux, CLS, Toulouse, IDS AWG Meeting, France, May 2015). An unmodeled change in satellite attitude on SPOT-5 might be one possible cause for the local peak in the SPOT-5 scale.

As shown by the summary of the single-satellite scales in Table 13, a second observation is that we have two families of scales: Envisat, SPOT-2 and TOPEX have mean scales

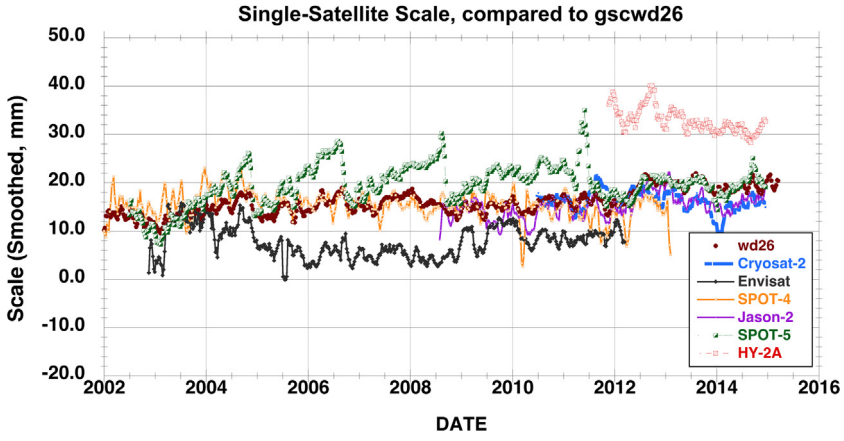

Fig. 19. Smoothed scale w.r.t. DPOD2008 for single-satellite coordinate solutions from 2002/0616 to 2014/1228 compared to the combination solution, gscwd26 for Cryosat-2, Envisat, HY-2A Jason-2, SPOT-4, and SPOT-5. The smoothed scale is computed using a five week running mean.

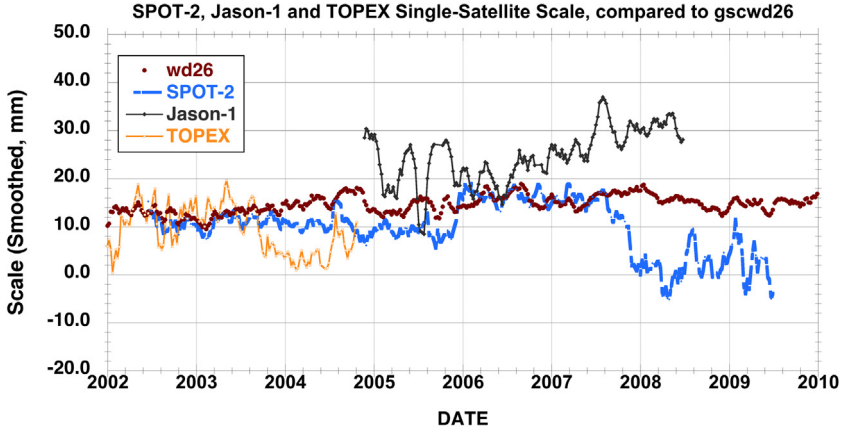

Fig. 20. Smoothed scale w.r.t. DPOD2008 for single-satellite coordinate solutions from 2002/0616 to 2009/0712 compared to the combination solution, gscwd26 for Jason-1, TOPEX, and SPOT-2. The smoothed scale is computed using a five week running mean.

Table 13
Scale of the single-satellite coordinate solutions for the period after 2002/0616, w.r.t. DPOD2008, compared to the full combination solution, gscwd26. In this table, we have smoothed the weekly scale estimates with a five week moving average.

Satellite	Dates	Single satellite	WRMS (mm)	
	(YY/MMDD)	scale (mm)	Satellite	gscwd26
Cryosat-2	2010/0606–2014/1228	16.29 ± 2.16	13.69	9.82
Envisat	2002/0616–2012/0325	7.71 ± 3.27	20.04	9.18
HY-2A	2011/1106–2014/1228	32.88 ± 2.49	18.16	10.15
Jason-1	2004/1107–2008/0706	24.73 ± 5.63	29.82	8.50
Jason-2	2008/0713–2014/1228	15.14 ± 2.44	20.57	10.55
SPOT-2	2002/0616–2009/0712	9.89 ± 5.37	21.05	9.10
SPOT-4	2002/0616–2013/0609	15.39 ± 2.69	18.64	9.22
SPOT-5	2002/0616–2014/1228	19.59 ± 4.20	14.00	9.41
TOPEX	2002/0616–2004/1031	9.11 ± 4.91	31.75	9.99
gscwd26	1993/0103–2014/1228	14.00 ± 3.43	–	11.74
gscwd26	2002/0616–2014/1228	16.04 ± 2.54	–	9.50

of 7–9 mm, whereas Cryosat-2, Jason-2, SPOT-4, SPOT-5 have mean scales of 15–19 mm. Both Jason-1 and HY-2A are outliers to these two groups. A third observation is that the scale of Jason-1 undergoes periodic oscillations that seem to have a period close to the draconitic period (117 days), but more worryingly shows a secular increase in scale after ~2006.5. SPOT-2 has two "jumps" in scale: +10 mm near 2006.0 and −15 to −18 mm towards the end of 2007. It would be worthwhile to verify that a change in on-board programming or DORIS station selection for SPOT-2 is or is not the origin of these jumps in the single-satellite scale.

A final observation is that the HY-2A scale is offset by +10–17 mm from the scale of the other DORIS satellites. A scale offset of this magnitude might be the signature of an error in the definition of the 2 GHz phase center for HY-2A or an error in the definition of the coordinates of the center of mass in the spacecraft frame, as found by Zelensky et al. (2016) for Saral. Gao et al. (2015) analyze HY-2A DORIS data using both the Doppler and the RINEX formulation, and also estimate a change in the Z (radial) offset of +1 to +1.25 cm (Gao et al., 2015, see Fig. 7). However, their a priori values of center of mass and definition of the 2 GHz phase center are completely different from those specified by Cerri and Ferrage (2013), so their results are hard to interpret. Whereas Cerri and Ferrage (2013) imply a vector from the center of mass to the 2 GHz phase center of +1305.2 mm, Gao et al. (2015) quote values which yield a vector of +1317.2 mm. The source of the discrepancy is not clear as the Cerri and Ferrage (2013) values were provided by the China National Space Agency (Alexandre Couhert, CNES, Toulouse, personal communication, July 2015). We may conclude that there is some uncertainty in the definition of fundamental geodetic tracking parameters for HY-2A that require clarification.

We summarize the statistics of the scale for the gscwd26 and the single-satellite solutions in Table 13. Therein, we tabulate the WRMS from the single satellite solutions, compared to the combination solution, gscwd26. TOPEX and SPOT-2, being the satellites with the first-generation DORIS receivers exhibit the highest scatter in the DORIS scales (as measured by their standard deviations). The Jason-1 single-satellite scale also has a higher scatter since for this test the SAA-related stations were not reduced. The satellites equipped with the DGXX receivers have a smaller scatter in their weekly scales. Concerning the WRMS, it is the SPOT-5 and Cryosat-2 satellites with the lowest single-satellite WRMS. Both TOPEX and Jason-1 have the highest single-satellite RMS, perhaps by virtue of their orbit inclination which may degrade the observability by these satellites for DORIS stations at the near-polar latitudes.

6.4. Earth orientation parameters

We evaluated the quality of the Earth orientation parameters for the gscwd26 series by comparing our DORIS-only-derived Earth orientation parameters with the IERS C04 series (Bizouard and Gambis, 2005). We adjusted the polar motion, Px and Py. The free-network solutions were transformed to the ITRF2008 reference after computing the full set of Helmert parameters. We compared the polar motion, Px and Py by time period after interpolating the IERS series (referenced at 0 h UT) to the time tag of the EOP in gscwd26 (referenced at 12 h UT). Since the information content of the DORIS station coordinate and EOP solutions depends so strongly on the number of satellites and the types of DORIS receivers (c.f. Moreaux et al., 2016), we divided the data into four time periods: (1) 1993/0103 to 2002/0612 (before the incorporation of the Envisat and SPOT-5 data); 2002/0613 to 2008/0712 (ending before the addition of data from Jason-2); (3) 2008/0713 to 2010/0605 (ending before the incorporation of Cryosat-2), and (4) 2010/0606 to 2014/1231.

A spectral analysis indicated that an annual term was present in the EOP for the first three time periods but absent in the final time period, where signals near

~256 days and ~186 days were present. For the final time period, the first periodic signal (~256 days) appears to be a sub-harmonic of the Cryosat-2 draconitic period, and the second periodic signal appears to be a sub-harmonic of the draconitic period for the sun-synchronous satellites. We fit an offset, drift and annual term to the differences with IERSC04 for the first three time periods, and an offset, drift and two periodic terms to the EOP differences for the final time period. We iteratively rejected EOP differences as outliers using a 3.5-sigma edit criterion. We report the RMS of these "residual differences" in Table 14 by time period for both polar motion, Px and Py. For the first time period (1993–2002) we find RMS differences with IERSC04 of 718 μarcsecs (μas) and 831 μas for Px and Py respectively, with only 63–68 points rejected as outliers out of a total of 8169 EOP estimates. For the second time period (2002–2008), we find RMS differences with IERSC04 of 442 μas and 509 μas for Px and Py respectively, rejecting only 14–18 points out of a total of 3453 EOP estimates. The best results are obtained for the Cryosat-2 time period (2010–2014), with RMS differences of 368 μas and 372 μas, where we reject 11–14 outliers out of 1670 EOP estimates. Although, the spectral analysis suggested peaks at periods of 256 days and 186 days, estimating fits to these harmonics instead of the annual terms for the fourth time period did not reduce the RMS in the EOP difference residuals. We note that estimating an annual harmonic in the differences reduced the variance for the first two time periods by only 15–20 μas, and by only 2–5 μas in the third and fourth time periods.

If we compare the RMS of the EOP differences with IERSC04 (after adjusting a trend and annual term) for the gscwd25 SINEX series compared to the gscwd26 series, we find that the strategy for adjusting the cross-track empirical accelerations less frequently reduced the RMS disagreement with IERSC04 by 30–36 μas for the period 1993 to 2002, by 15–24 μas for the period 2002 to 2008, and by 5–10 μas for 2008 to 2010 (after the introduction of Jason-2 and before the addition of Cryosat-2).

The gscwd26 EOP are clearly noisier than those of the IDS combination, where (Moreaux et al., 2016, (see Table 9)) obtains standard deviations of the differences with IERSC04 (after fitting a bias and a trend) of 245 and 235 μas for Px and Py. It is possible that estimation strategy of not applying a priori constraints on the estimation of any of the arc parameters (including the numerous pass-by-pass troposphere parameters and range-rate biases) may weaken the determination of the EOP in the gscwd26 solution.

7. Summary

In this paper we have summarized the processing of 21 years of DORIS data, from 1993.0 to 2015.0 in order to develop the NASA GSFC DORIS contribution to ITRF2014. We have demonstrated an improvement in the quality of the station coordinate solutions compared to ITRF2008, as measured by the WRMS, and the behavior of the scale and translation parameters associated with the weekly solutions. We have successfully reprocessed all the data incorporated into ITRF2008 (Le Bail et al., 2010), and have added data from four satellites: Jason-1, Jason-2, Cryosat-2, and HY-2A. The addition of the new satellites necessitated a separate and detailed verification of the attitude models, which was facilitated with the joint analysis of both SLR and DORIS data. We implemented a series of improvements to the force modeling and to the measurement modeling in a step-wise basis, using interim SINEX series to validate the results. For the force model, the most important improvements included corrections to

Table 14
Earth orientation parameter differences with IERS C04 series (in μ as (micro-arcseconds)).

Dates	Fit Used	Px, RMS (μas)	Px (npts)	Py, RMS (μas)	Py (npts)
1993/0103 – 2014/1231	Mean‡	640	8169	728	8169
	Trend	580	8106	652	8104
	Trend + Annual	564	8101	645	8106
1993/0103 – 2002/0612	Mean‡	772	3453	867	3453
	Trend	737	3429	851	3437
	Trend + Annual	718	3429	831	3435
2002/0613 – 2008/0712	Mean‡	487	2219	559	2219
	Trend	463	2208	526	2204
	Trend + Annual	442	2201	509	2205
2008/0713 – 2010/0605	Mean‡	389	691	417	693
	Trend	384	690	412	693
	Trend + Annual	382	690	407	692
2010/0606 – 2014/1231	Mean‡	472	1670	408	1670
	Trend	373	1656	376	1659
	Trend + Annual	368	1656	372	1659
	Trend + 256 d + 186 d	374	1657	372	1659

‡ No edits.

or a retuning of the macromodels for SPOT-2, SPOT-3, and Envisat, as well as the use of more detailed modeling of time-variable gravity using a series of weekly spherical harmonic solutions, overlain on an improved GRACE and GOCE-derived gravity model, GOCO2S (Goiginger et al., 2011). For the measurement model, the three most important changes concerned: (1) the modification of the estimation strategy to account for the difference in the beacon frequency from the nominal value; (2) the application of the GEODYN-computed antenna offset corrections in conjunction with the use of satellite attitude data (quaternions) or an internal attitude model; (3) the application of the Starec and Alcatel antenna phase laws. In terms of changes in parameterization, we have applied for TOPEX the DORIS system time-biases determined from SLR and DORIS orbit determination solutions, and we adopted a strategy of reducing the frequency of adjustment for the cross-track accelerations.

In conducting the analysis of DORIS data in fine detail, we have illuminated issues that will need to be addressed in order to continue to improve the quality of the DORIS stations coordinate and EOP solutions. The most perplexing issues relate to the strange patterns that we observe in the scales of single-satellite SINEX solutions. These include (1) the 'sawtooth' pattern in the SPOT-5 scales; (2) the offsets in the scale for some satellites (HY-2A); (3) the periodic behavior and secular increase in scale for Jason-1. While the issues with HY-2A are likely due to an incorrect definition of the center of mass or of the DORIS 2 GHz offset, no ready explanation is available for the phenomena observed on Jason-1 and SPOT-5.

An additional issue of concern is to what extent the satellites, which we do not provide spacecraft-derived attitude information, follow the prescribed attitude laws. We have evidence in at least one case for a short time, for both SPOT-4 and SPOT-5 (see Section 4.2.2) that the RMS of fit is degraded if we apply the prescribed attitude model in the computation of the antenna offset corrections. In addition, we note that for SPOT-2, the amplitude of the daily along-track empirical accelerations are noticeably different after 2002, compared to before 1999. The SPOT project has not reported any change in the pitch of the spacecraft solar array (Pascale Ferrage, CNES, Toulouse, France, personal communication, July 2015), so we must seek an alternate explanation for this behavior on SPOT-2 and adapt the satellite modeling accordingly. It would be highly desirable for current or future satellite missions if spacecraft attitude information (that specifies the rotation from the spacecraft to the interial J2000 reference frame) were made available on a systematic basis. Presently this information is not publically available for Saral, HY-2A, and the SPOT satellites.

We have used detailed macromodels for all the satellites, with the exception of Envisat and Jason-1 where we used the radiation pressure models developed by University College London (UCL) (Ziebart, 2004; Sibthorpe, 2006). The macromodels do not necessarily account for self-shadowing (c.f., see Mazarico et al., 2009) or all aspects of radiation interactions with the surfaces of a satellite, so there is further room for improvement. In this work and that of Moreaux et al. (2016), the EOP remain contaminated with large signals at the annual periods (draconitic periods for the sun-synchronous satellites) over some portions of the time series, and smaller signals at other periods. A goal should be to see if improved surface force modeling can reduce these systematic signals in the DORIS EOP, and if changes in estimation strategy can improve the EOP quality.

Acknowledgements

We acknowledge the International DORIS Service and the International Laser Ranging Service for providing the SLR and DORIS data that we have used (Pearlman et al., 2002; Willis et al., 2010). We thank the GEODYN team at the NASA Goddard Space Flight Center for their contributions throughout the course of our work as we processed data and prepared the solutions for ITRF2014, including Despina E. Pavlis (SGT Inc) and Jesse Wimert (SGT Inc.). We acknowledge Guilhem Moreaux (Collecte Localisation Satellites; IDS Combination Center Toulouse, France) for the many analyses, tests and exchanges that have allowed us to refine and improve our solutions.

This work was suppported by the U.S. National Aeronautics and Space Administration, under following the programs: Interdisciplinary Research in Earth Science, Ocean Surface Topography Science Team (OSTST), and Making Earth System data records for Use in Research Environments (MEaSUREs).

Appendix A. Supplementary data

Supplementary data associated with this article can be found, in the online version, at http://dx.doi.org/10.1016/j.asr.2015.12.043.

References

Altamimi, Z., Collilieux, X., Métivier, L., 2011. ITRF2008: an improved solution of the international terrestrial reference frame. J. Geod. 85 (8), 457–473. http://dx.doi.org/10.1007/s00190-011-0444-4.

Auriol, A., Tourain, C., 2010. DORIS system: the new age. Adv. Space Res. 46 (12), 1484–1496. http://dx.doi.org/10.1016/j.asr.2010.05.015.

Belli, A., Exertier, P., Samian, E., Courde, C., et al., 2015. Characterization of an ultra stable quartz oscillator thanks to Time Transfer by Laser Link (T2L2, Jason-2). In: Frequency Control Symposium and the European Frequency and Time Forum (FCS), 2015 Joint Conference of the IEEE International (Proceedings of), Denver, Colorado, 12–16 April 2015, pp. 808–812, 2015, doi:10.1109/FCS.2015.7138964.

Bizouard, C., Gambis, D., 2005. The combined solution C04 for earth orientation parameters consistent with international terrestrial reference frame. In: Drewes, H. (Ed.), Geodetic Reference Frames, IAG Symp., vol. 134. Springer-Verlag, Berlin, pp. 265–270. http://dx.doi.org/10.1007/978-3-642-00860-341.

Boehm, J., Schuh, H., 2004. Vienna mapping functions in VLBI analyses. Geophys. Res. Lett. 31, L01603. http://dx.doi.org/10.1029/2003GL018984.

Boehm, J., Niell, A., Tregoning, P., Schuh, H., 2006. Global mapping function (GMF): a new empirical mapping function based on

numerical weather model data. Geophys. Res. Lett. 33, L07304. http://dx.doi.org/10.1029/2005GL025546.

Boehm, J., Heinkelmann, R., Schuh, H., 2007. Short note: a global model of pressure and temperature for geodetic applications. J. Geod. 81 (10), 679–683. http://dx.doi.org/10.1007/s00190-007-0135-3.

Bruinsma, S., 2014. The semi-empirical thermosphere model DTM2013 (Drag Temperature Model), IDS Workshop, Konstanz, Germany, October 27–28, 2014, http://ids-doris.org/images/documents/report/idsworkshop2014/IDS14s4BruinsmaDTM2013thermosphereModel.pdf.

Bruinsma, S., Lemoine, J.M., Biancale, R., Valès, N., 2010. CNES/GRGS 10-day gravity field models (release 02) and their evaluation. Adv. Space Res. 45 (4), 587–601. http://dx.doi.org/10.1016/j.asr.2009.10.012.

Bruinsma, S.L., Sánchez-Ortiz, N., Olmedo, E., Guijarro, N., 2012. Evaluation of the DTM-2009 thermosphere model for benchmarking purposes. J. Space Weather Space Climate 2 (A04). http://dx.doi.org/10.1051/swsc/2012005.

Capdeville, H., Lemoine, J.M., Štěpánek, P., 2016. Update of the corrective model for Jason-1 DORIS data in relation to the South Atlantic Anomaly and a corrective model for Spot-5. Adv. Space Res. 58 (12), 2628–2650.

Cerri, L., Ferrage, P., 2013. DORIS satellite models implemented in POE processing, CNES document SALP-NT-BORD-OP-16137-CN, Rev. 5, Toulouse, France, July 15, 2013 ftp://ftp.ids-doris.org/pub/ids/satellites/DORISSatelliteModels.pdf.

Cerri, L., Berthias, J.P., Bertiger, W.I., et al., 2010. Precision orbit determination standards for the Jason series of altimeter missions. Marine Geod. 33 (1), 379–418. http://dx.doi.org/10.1080/01490419.2010.488966.

Couhert, A., Cerri, L., Lemoine, J.-M., et al., 2015. Towards the 1 mm/y stability of the radial orbit error at regional scales. Adv. Space Res. 55 (1), 2–23. http://dx.doi.org/10.1016/j.asr.2014.06.041.

Förste, C., Schmidt, R., Stubenvoll, R., et al., 2008. The GeoForschungsZentrum Potsdam/Groupe de Recherche de Géodésie Spatiale satellite-only and combined gravity field models: EIGEN-GL04S1 and EIGEN-GL04C. J. Geod. 82 (6), 331–346. http://dx.doi.org/10.1007/s00190-007-0183-8.

Gao, F., Peng, B., Zhang, Y., et al., 2015. Analysis of HY2A precise orbit determination using DORIS. Adv. Space Res. 55 (5), 1394–1404. http://dx.doi.org/10.1016/j.asr.2014.11.032.

Gitton, P., Kneib, J., 1990. Influence of the surface forces on the orbit of the SPOT satellite. Internal Report. Colorado Center for Astrodynamics Research, University of Colorado, Boulder, July 1990, http://ids-doris.org/documents/report/publications/StudyReport-1990-SpotSatelliteSurfaceForces-GittonKneib.pdf.

Gobinddass, M.L., Willis, P., de Viron, O., et al., 2009. Improving DORIS geocenter time series using an empirical rescaling of solar radiation pressure models. Adv. Space Res. 44 (11), 1279–1287. http://dx.doi.org/10.1016/j.asr.2009.08.004.

Goiginger, H., Rieser, D., Mayer-Gürr, T., et al., 2011. he combined satellite-only global gravity field model GOCO02S. Geophys. Res. Abstr. 13, EGU2011-10571, 2011. http://www.goco.eu/data/egu2011-10571-goco02s.pdf.

Hedin, A.E., 1987. MSIS-86 thermospheric model. J. Geophys. Res. 92 (A5), 4649–4662. http://dx.doi.org/10.1029/JA092iA05p04649.

IERS, 2013. (International Earth Rotation and Reference System Service) Message 225, ITRF2013 Call for Participation, http://www.iers.org.

Le Bail, K., Lemoine, F.G., Chinn, D.S., 2010. GSFC DORIS contribution to ITRF2008. Adv. Space Res. 45 (12), 1481–1499. http://dx.doi.org/10.1016/j.asr.2010.01.030.

Lemoine, J.M., Capdeville, H., 2006. A corrective model for Jason-1 DORIS Doppler data in relation to the South Atlantic Anomaly. J. Geod. 80 (8), 507–523. http://dx.doi.org/10.1007/s00190-006-0068-2.

Lemoine, F., Chinn, D., Zelensky, N., Beall, J., 2014. Time-variable gravity solutions from 1993 to 2014 from SLR and DORIS data, Abstract G23A–0472, American Geophysical Union Fall Meeting, San Francisco, California, December 15–19, 2014, http://ids-doris.org/images/documents/report/publications/AGU2014-TVGsolutionsFromSLRandDORISdata-Poster-Lemoine.pdf.

Lemoine, F.G., Zelensky, N.P., Chinn, D.S., Beckley, B.D., Lillibridge, J. L., 2006. Towards the GEOSAT Follow-On precise orbit determination goals of high accuracy and near-real-time processing. In: AIAA Paper 2006–6402, AIAA/AAS Astrodynamics Conference, 21–24 August 2006, Keystone, Colorado. (http://arc.aiaa.org/doi/abs/10.2514/6.2006-6402).

Lemoine, F.G., Zelensky, N.P., Chinn, D.S., et al., 2010. Towards development of a consistent orbit series for TOPEX, Jason-1, and Jason-2. Adv. Space Res. 46 (12), 1513–1540. http://dx.doi.org/10.1016/j.asr.2010.05.007.

Marshall, J.A., Zelensky, N.P., Klosko, S.M., et al., 1995. The temporal and spatial characteristics of TOPEX/Poseidon radial orbit error. J. Geophys. Res. 100 (C12), 25331–25352. http://dx.doi.org/10.1029/95JC01845.

Mazarico, E., Zuber, M.T., Lemoine, F.G., 2009. Effects of self-shadowing on nonconservative force modeling for Mars-Orbiting spacecraft. J. Spacecraft Rockets 46 (3), 662–669. http://dx.doi.org/10.2514/1.41679.

Moreaux, G., Lemoine, F.G., Capdeville, H., Kuzin, S., Otten, M., Štěpánek, P., Willis, P., Ferrage, P., 2016. The International DORIS Service contribution to the 2014 realization of the International Terrestrial Reference Frame. Adv. Space Res. 58 (12), 2479–2504. http://dx.doi.org/10.1016/j.asr.2015.12.021.

Niell, A.E., 1996. Global mapping functions for the atmosphere delay at radio wavelengths. J. Geophys. Res. 101 (B2), 3227–3246. http://dx.doi.org/10.1029/95JB03048.

Noll, C., Soudarin, L., 2006. On-line ressources supporting the data, products, and information infrastructure for the International DORIS Service. J. Geod. 80 (8), 419–427. http://dx.doi.org/10.1007/s00190-006-0051-y.

Pavlis, D.E., Wimert, J., McCarthy, J.J., 2015. GEODYN II system description, Vol. 1–5, contractor report, SGT Inc., Greenbelt, Maryland, U.S.A.

Pearlman, M.R., Degnan, J.J., Bosworth, J.M., 2002. The international laser ranging service. Adv Space Res. 30 (2), 135–143. http://dx.doi.org/10.1016/S0273-1177(02)00277-6.

Petit G., Luzum, B., 2010. IERS conventions 2010. IERS technical Note 36, Verlag des Bundesamts für Kartographie und Geodäsie, ISBN 3-89888-989-6, Frankfurt am Main, Germany, http://www.iers.org/TN36.

Ray, R., 2013. Precise comparisons of bottom-pressure and altimetric ocean tides. J. Geophys. Res. Oceans 118, 4570–4584. http://dx.doi.org/10.1002/jgrc.20336.

Rudenko, S., Dettmering, D., Esselborn, S., et al., 2014. Influence of time variable geopotential models on precise orbits of altimetry satellites, global and regional sea level trends. Adv. Space Res. 54 (1), 92–118. http://dx.doi.org/10.1016/j.asr.2014.03.010.

Sibthorpe, A., 2006. Precision non-conservative force modelling for low Earth orbiting spacecraft (Ph.D. Thesis), University College London (UCL), London, UK.

Štěpánek, P., Dousa, J., Filler, V., 2013. SPOT-5 DORIS oscillator instability due to South Atlantic Anomaly: mapping the effect and application of data corrective model. Adv. Space Res. 52 (7), 1355–1365. http://dx.doi.org/10.1016/j.asr.2013.07.010.

Štěpánek, P., Rodrigruez-Solano, C.J., Hugentobler, U., Filler, V., 2014. Impact of orbit modeling on DORIS station position and Earth rotation estimates. Adv. Space Res. 53 (7), 1058–1070. http://dx.doi.org/10.1016/j.asr.2014.01.007.

Tourain, C., Moreaux, G., Auriol, A., Saunier, J., 2016. DORIS Starec ground antenna characterization and impact on positioning. Adv. Space Res. 58 (12), 2707–2716.

Willis, P., Fagard, H., Ferrage, P., et al., 2010. The international DORIS service (IDS): toward maturity. Adv. Space Res. 45 (12), 1408–1420. http://dx.doi.org/10.1016/j.asr.2009.11.018.

Willis, P., Zelensky, N.P., Ries, J., et al., 2015. DPOD2008, a DORIS-oriented terrestrial reference frame for precise orbit

determination. IAG Symp. Ser. 143. http://dx.doi.org/10.1007/13452015125.

Zelensky, N.P., Berthias, J.P., Lemoine, F.G., 2006. DORIS time bias estimated using Jason-1, TOPEX/Poseidon and Envisat orbits. J. Geod. 80 (8), 497–506. http://dx.doi.org/10.1007/s00190-006-0075-3.

Zelensky, N.P., Lemoine, F.G., Ziebart, M., et al., 2010a. DORIS/SLR POD modeling improvements for Jason-1 and Jason-2. Adv. Space Res. 46 (12), 1541–1558. http://dx.doi.org/10.1016/j.asr.2010.05.008.

Zelensky, N.P., Lemoine, F.G., Chinn, D.S., Pavlis, D.E., Rowlands, D. D., Le Bail, K., 2010b. Improving DORIS troposphere modeling for Jason-1 and Jason-2, IDS Workshop, Lisbon, Portugal, October 21–22, 2010, http://ids-doris.org/images/documents/report/idsworkshop2010/IDS10s4ZelenskyTroposphereMeasurementsJason.pdf.

Zelensky N.P., Lemoine, F.G., Chinn, D.S., et al., 2011. Time varying gravity modeling for precise orbits across the TOPEX/Poseidon, Jason-1 and Jason-2 Missions, Poster, Ocean Surface Topography Science Team Meeting, San Diego, California, http://www.aviso.oceanobs.com/fileadmin/documents/OSTST/2011/poster/zelenskypod5.pdf.

Zelensky, N.P., Lemoine, F.G., Chinn, D.S., 2016. Towards the 1-cm Saral orbit. Adv. Space Res. 58 (12), 2651–2676. http://dx.doi.org/10.1016/j.asr.2015.12.011.

Ziebart, M., 2004. Generalized analytical solar radiation pressure modeling algorithm for spacecraft of complex shape. J. Spacecraft Rockets 41 (5), 840–848. http://dx.doi.org/10.2514/1.13097.